Inclusive W & Z measurements in CMS

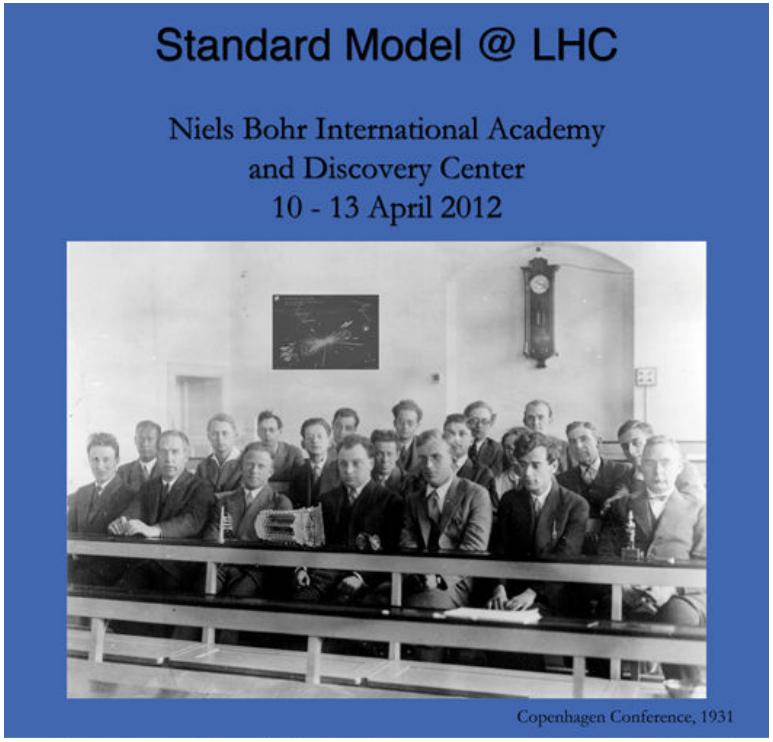

Georgios Daskalakis
N.C.S.R. "Demokritos"

on behalf of CMS Collaboration

Overview

LHC hopefully will be proven to be a discovery machine but before that the measurement of the known "unknowns" in the new Energy frontier :

- is an excellent way to understand and commission "physics objects".
- provides a good understanding of SM processes improving our knowledge on PDFs, pQCD, UE modeling …
- in most of the cases SM processes are backgrounds to searches for new Physics, so SM measurements are themselves by default "searches".

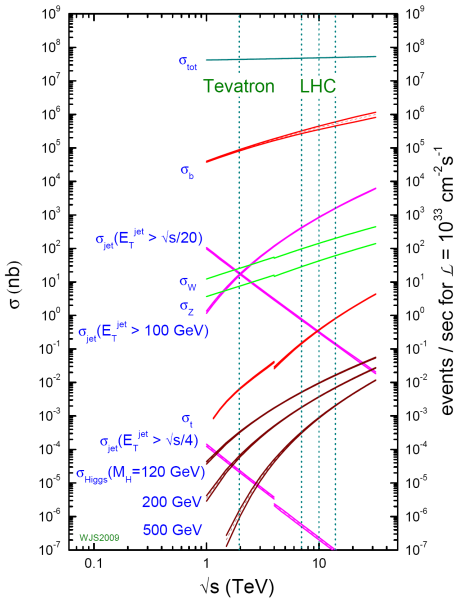

W & Z productions are theoretically well understood, have high rates and distinctive signatures.

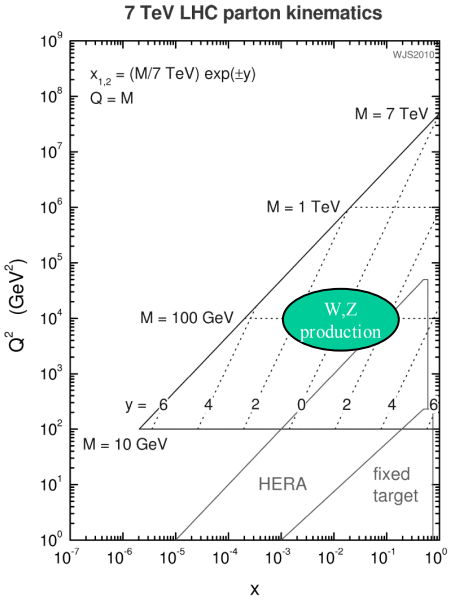

Today I 'll report on:

- W & Z inclusive cross section measurements and ratios in e,μ,τ final states.
- W charge asymmetry & W polarization measurements.
- Z rapidity and transverse momentum measurements.
- Differential dσ/dM and double differential $d^2\sigma/dMdY$ DY cross sections.
- Forward-Backward Asymmetry and Weak-mixing Angle from DY pairs.

W & Z production mechanisms

flavour decomposition of W cross sections

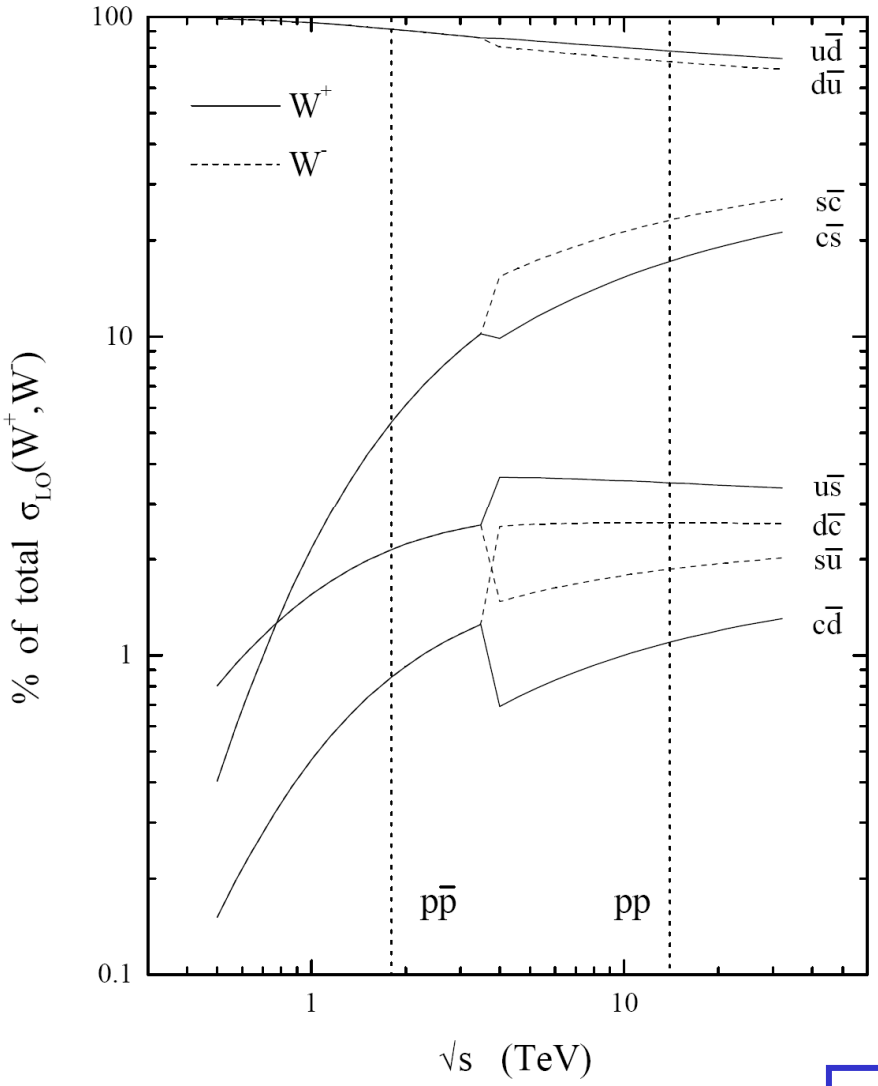

flavour decomposition of Z cross sections

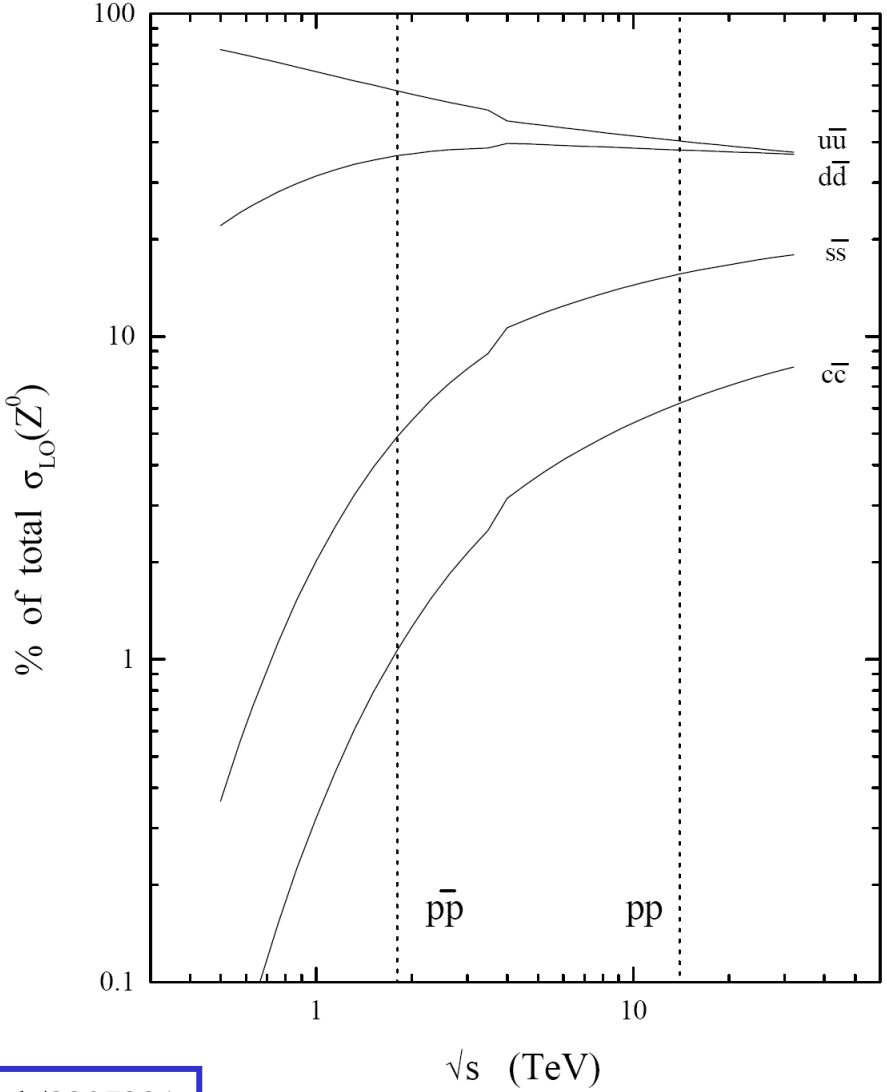

hep-ph/9907231

Selection of W & Z candidates (e , μ final states)

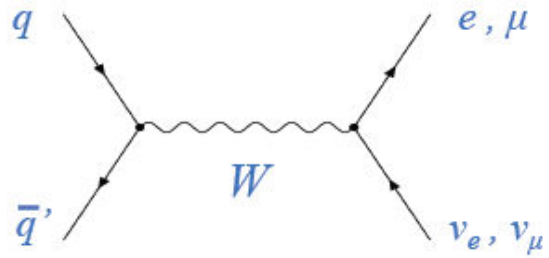

BACKGROUND
QCD multi-jets , γ+jets (electron)
$\gamma^*/Z \rightarrow e^+e^-$, $\mu^+\mu^-$, $\tau^+\tau^-$
$W \rightarrow \tau\nu$, tt, WW, WZ, ZZ

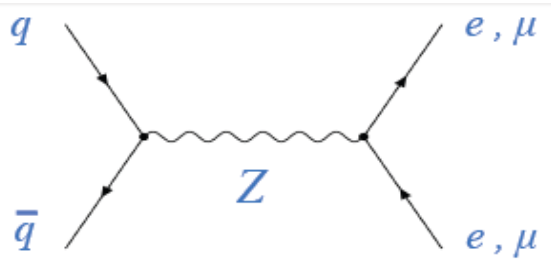

BACKGROUND
$\gamma^*/Z \rightarrow \tau^+\tau^-$, W+jets, tt,
WW, WZ, ZZ, QCD multi-jets

Electron & Muon selection:

W: high P_T lepton inside the fiducial volumes of the detector, isolated, tight e-ID or μ-ID, Z veto

Z: two high P_T leptons inside the fiducial volumes of the detector, isolated, tight e-ID or μ-ID

Signal yield extracted from

W: MET or isolation, with data-driven methods for the QCD bkgd estimation, EWK bkgds from MC

Z: di-lepton invariant mass (simple counting or fit)

Selection efficiency for signal falling within the acceptance

- Obtained from simulation
- Corrected using efficiencies measured in data and MC with a T&P technique

$$\varepsilon = \varepsilon_{MC} \times \rho_{eff}, \quad \rho_{eff} = \varepsilon_{T\&P}(\text{data}) / \varepsilon_{T\&P}(\text{MC})$$

Acceptance

Determined from simulation. Source of theoretical uncertainties.

Inclusive W cross section (36 pb^{-1})

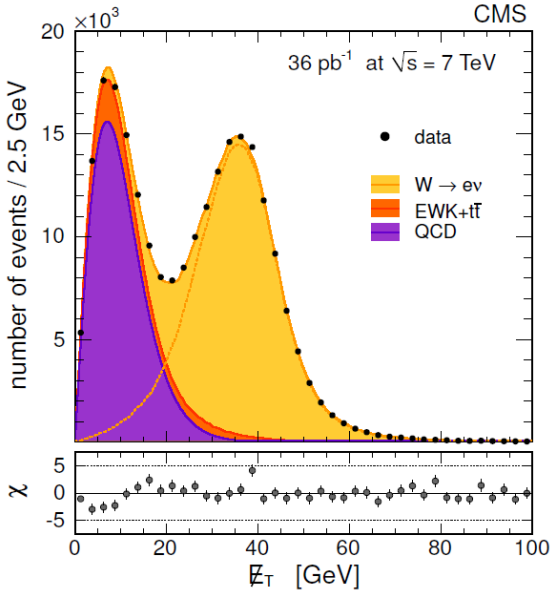

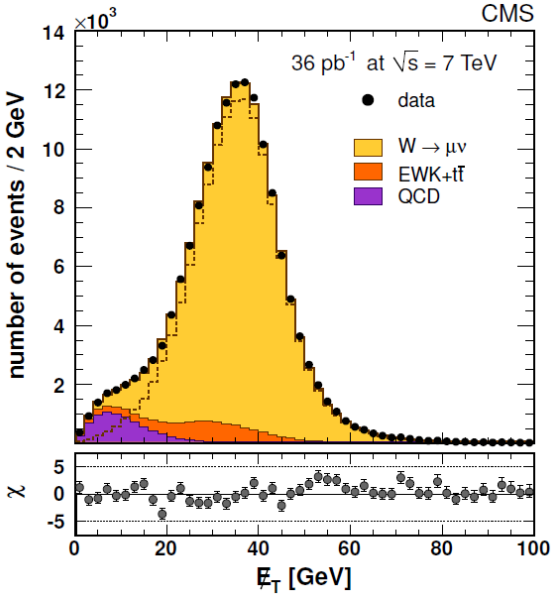

Electrons: E_T>25 GeV, |η|<2.5, 1.44<|η|<1.57 excl.
Muons: P_T>25 GeV, |η|<2.1
W→eν (μν): **Signal** 136 k (141 k) ; **Acc × Eff (%)** 36.3 (38.5)

Signal shape (W):
MC + Z→ll data for Recoil tuning

Signal extraction (W):
fits to missing transverse energy (MET) with templates or analytical functions, ABCD, matrix method

	W→eν (%)	**W→μν (%)**
Experimental	1.5	1.1
Theoretical	0.9	1.1
Total (Exp. + Th.)	**1.7**	**1.6**
Luminosity	4.0%	

Experimental : Lepton reconstruction & ID , Trigger pre-firing, Momentum/Energy scale & resolution, MET scale and resolution, Background subtraction/modeling.

Theoretical : PDF & HO corrections uncertainties on acceptance & MC efficiencies (POWHEG+CT10, PDF4LHC (68% CL) with [MSTW08, CT10, NNPDF2.0] , α_s errors, scale unc.)

Inclusive W cross section (36 pb^{-1})

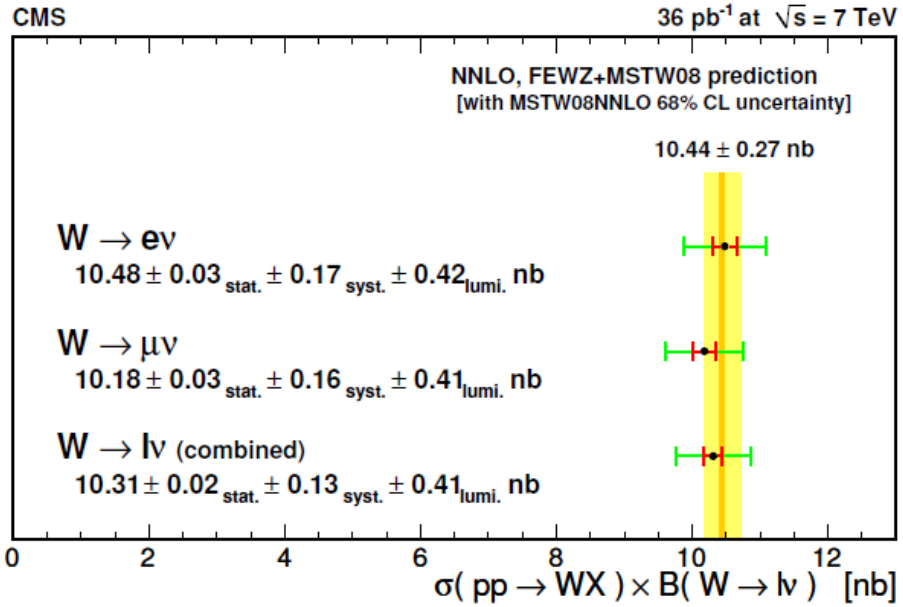

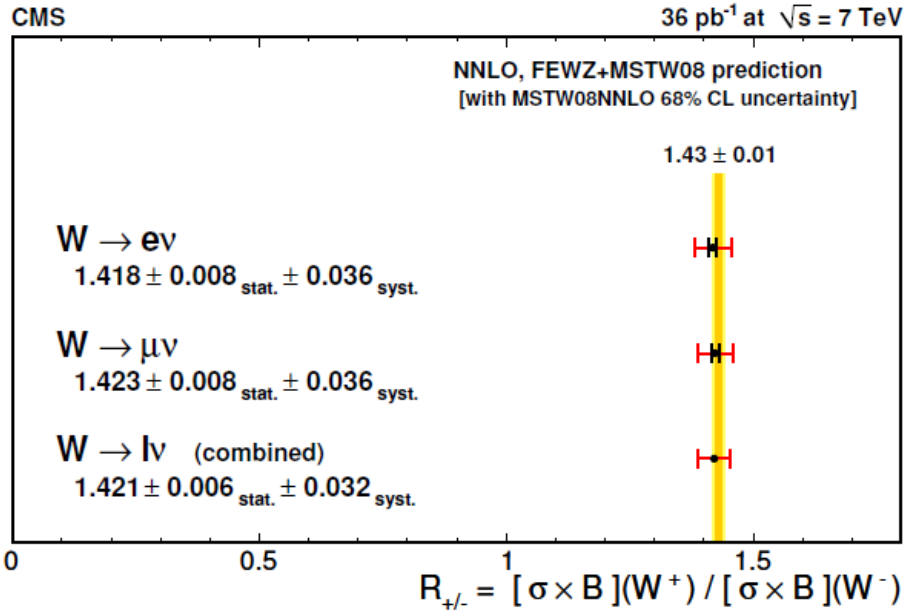

W$^+$/W$^-$ ratios agrees well with the NNLO FEWZ+MSTW08NNLO prediction.

W$^+$/W$^-$ ratio shows small dependence on NNLO vs NLO and the α_s value.

Important differences between different predictions at both NNLO and NLO PDFs.

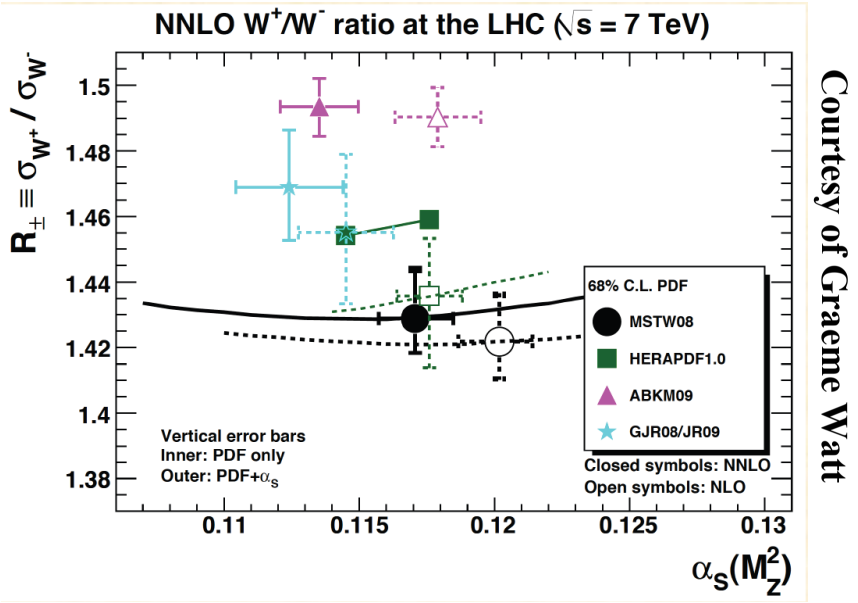

Inclusive $W \to \tau_{had} \nu$ cross section (32.4 pb^{-1})

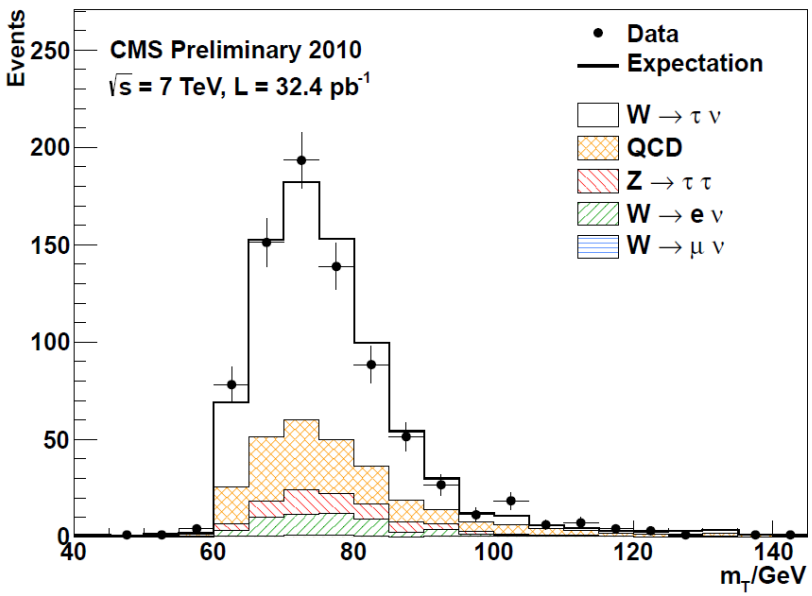

Tau leptons are identified via their **hadronic decays**.

Trigger : at least one hadronic tau decay + MET

Offline event selection:

- τ_{had} candidate $P_T > 30$ GeV, $|\eta|<2.3$
- PF MET > 30 GeV and CALO-MET > 25 GeV
- Veto of electron or muon of $P_T > 15$ GeV
- $M_T > 40$ GeV
- $P_T(\tau_{had})$ / (scalar sum of P_T of jets with $P_T > 15$ GeV and $|\eta|<3$) < 0.65

Acceptance ~ 8%, Efficiency ~3.3%

Backgrounds:
Data-driven QCD background estimation.
EWK backgrounds from MC.

Channel	$\sigma(pp \to WX) \times \mathcal{B}$ (nb)	NNLO (nb)
$W \to \tau\nu$	$8.96 \pm 0.51(\text{stat.})^{+2.32}_{-2.26}(\text{syst.}) \pm 0.36(\text{lumi.})$	10.44 ± 0.52
$W^+ \to \tau^+\nu$	$5.26 \pm 0.39(\text{stat.})^{+1.36}_{-1.29}(\text{syst.}) \pm 0.21(\text{lumi.})$	6.15 ± 0.29
$W^- \to \tau^-\nu$	$3.40 \pm 0.33(\text{stat.})^{+0.92}_{-0.93}(\text{syst.}) \pm 0.14(\text{lumi.})$	4.29 ± 0.23

$$R_{+/-} = \frac{\sigma(pp \to WX) \times \mathcal{B}(W^+ \to \tau^+\nu)}{\sigma(pp \to WX) \times \mathcal{B}(W^- \to \tau^-\nu)} = 1.55 \pm 0.19(\text{stat.})^{+0.11}_{-0.13}(\text{syst.})$$

1.43 ± 0.04 NNLO prediction

Source	Uncertainty
Trigger efficiency	15%
Tau–jet energy scale	$^{+16.0}_{-14.8}$%
Jet energy scale	$^{+10.0}_{-10.1}$%
PDF	4%
Luminosity	4%
Background contributions	10.1%
∑ Systematic Uncertainties	$^{+25.8}_{-25.1}$%

W Charge Asymmetry

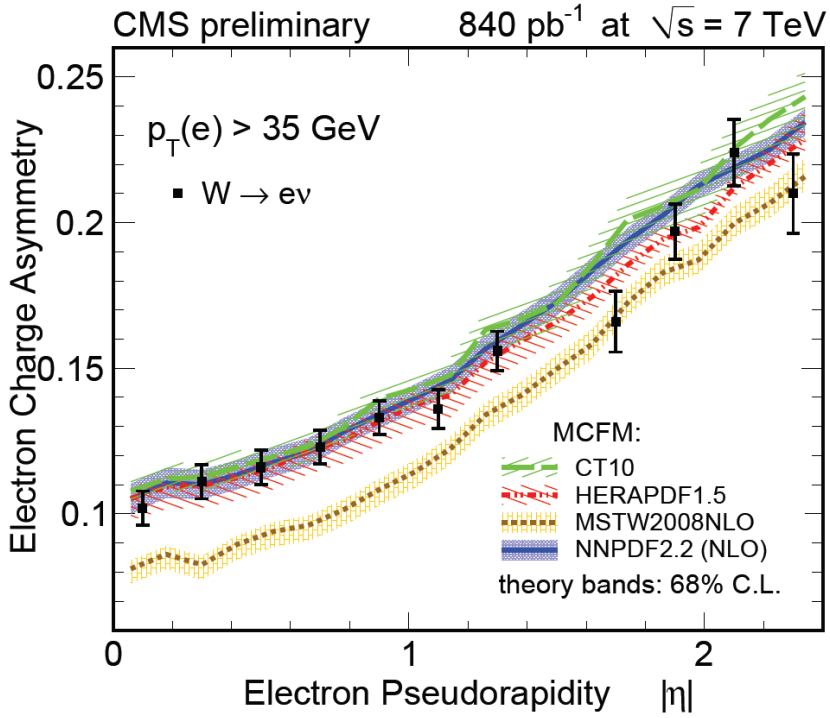

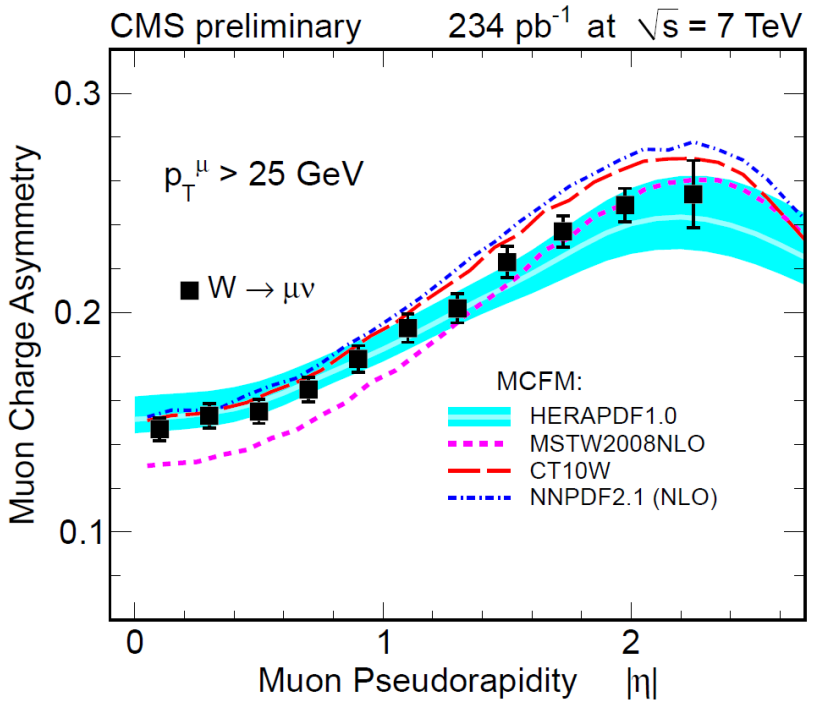

- Two valence u quarks in the proton ➔ overall excess of W^+ over W^-
- Charge asymmetry for electrons and muons agree with each other.
- Predictions from different PDF models don't agree each other within the PDF uncertainties.
- Precision of the measurement good enough to provide new inputs to the PDF global fits.
- Main systematic uncertainties:

  Signal estimation, possible efficiency differences between l^+ and l^-, lepton momentum (energy) scale and resolution, lepton charge misID.

W polarization (36 pb^{-1})

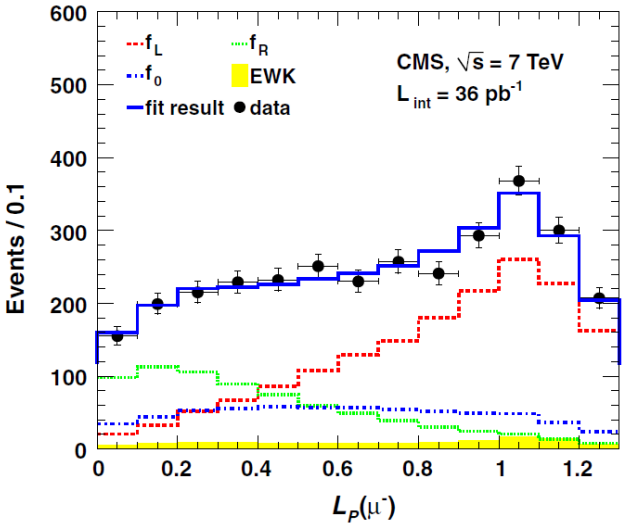

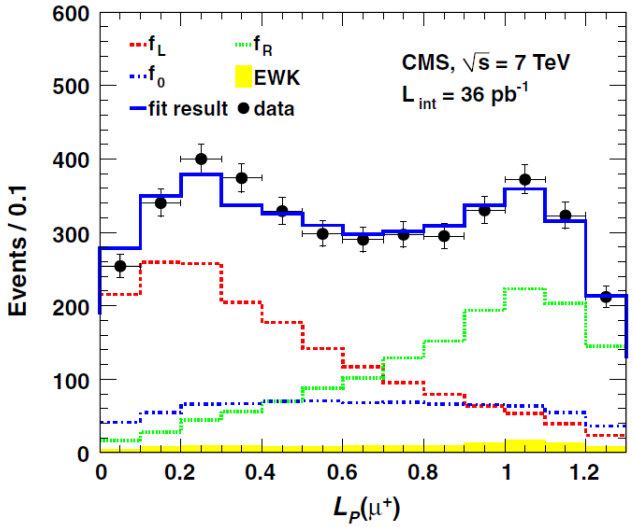

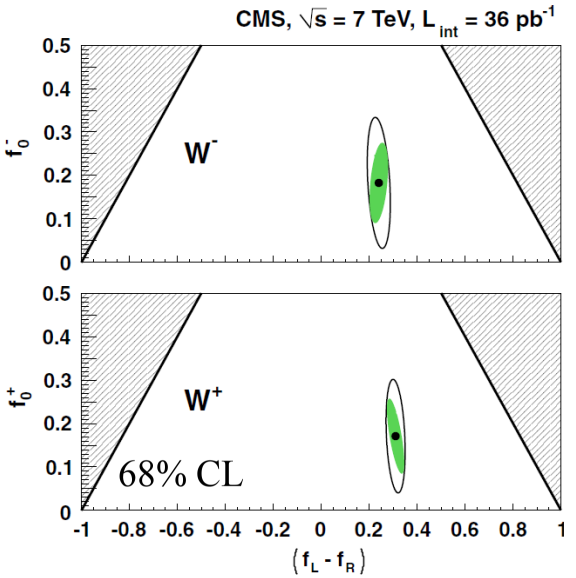

- Dominance of quark-gluon initial states plus V-A W-fermion coupling leads to significant polarization of W bosons with large transverse momenta (>50 GeV) in pp collisions.
- Exact value of polarization depends on the proportion of the qg, $\overline{q}$g, q$\overline{q}$ contributions, reflected in the helicity angle (cosθ*) distribution.
- Determination of the f_L, f_R, f_0 left-handed, right-handed and longitudinal polarization fractions in the W rest frame is experimentally inaccessible.
- L_p avoids ambiguity in cosθ* due to neutrino direction

$$L_P = \frac{\vec{p}_T(\ell) \cdot \vec{p}_T(W)}{|\vec{p}_T(W)|^2} \simeq \frac{1+\cos\theta^*}{2}$$

if $P_T(W) >> M_W$

Lepton projection (transverse plane)

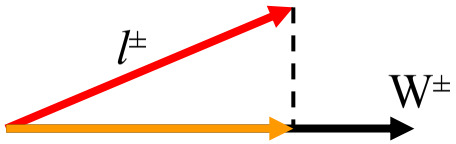

The measurement establishes that W bosons in pp collisions with large transverse momenta are **predominantly left-handed**, as expected in the Standard Model.

Inclusive Z cross section (36 pb^{-1})

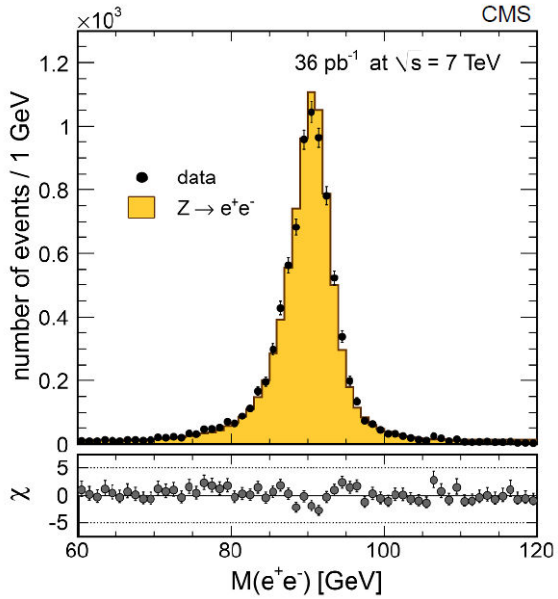

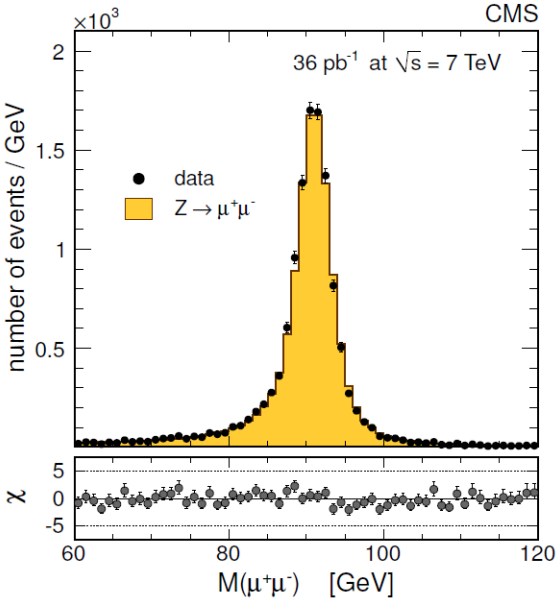

Electrons: E_T>25 GeV, |η|<2.5, 1.44<|η|<1.57 excl.
Muons: P_T>20 GeV, |η|<2.1
Z→ee (μμ): Signal 8.4 k (13.7 k) ; **Acc × Eff (%)** 23.6 (39.4)

Backgrounds: Almost negligible.

Signal extraction: Cut & count in 60<M_{ll}<120 GeV, Fits to M_{ll} for Signal yield and efficiencies.

	Z→ee (%)	**Z→μμ (%)**
Experimental	1.8	0.7
Theoretical	1.7	2.0
Total (Exp. + Th.)	**2.5**	**2.1**
Luminosity	4.0%	

Experimental : Lepton reconstruction & ID , Trigger pre-firing, Momentum/Energy scale & resolution, Background subtraction

Theoretical : PDF & HO corrections uncertainties on acceptance & MC efficiencies (POWHEG+CT10, PDF4LHC (68% CL) with [MSTW08, CT10, NNPDF2.0] , α_s errors, scale unc.)

Inclusive Z cross section (36 pb^{-1})

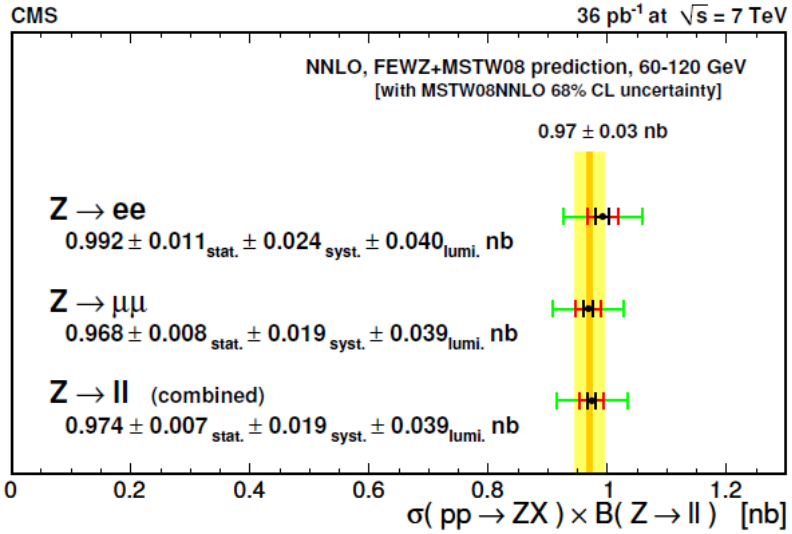

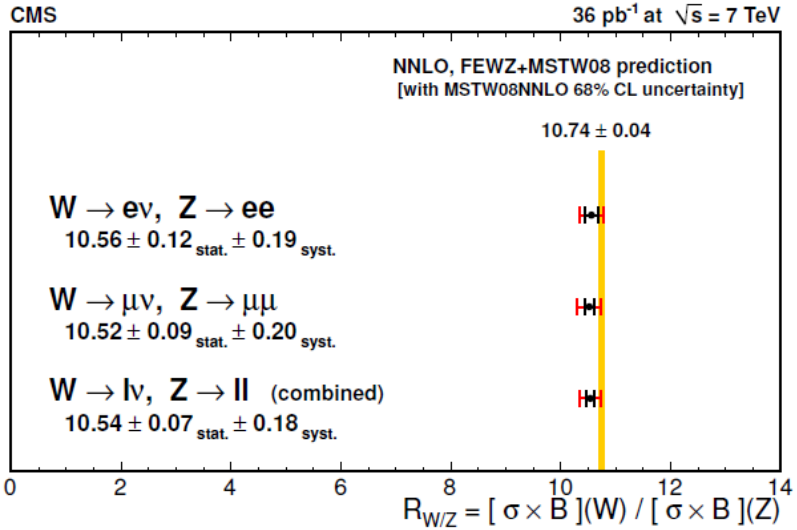

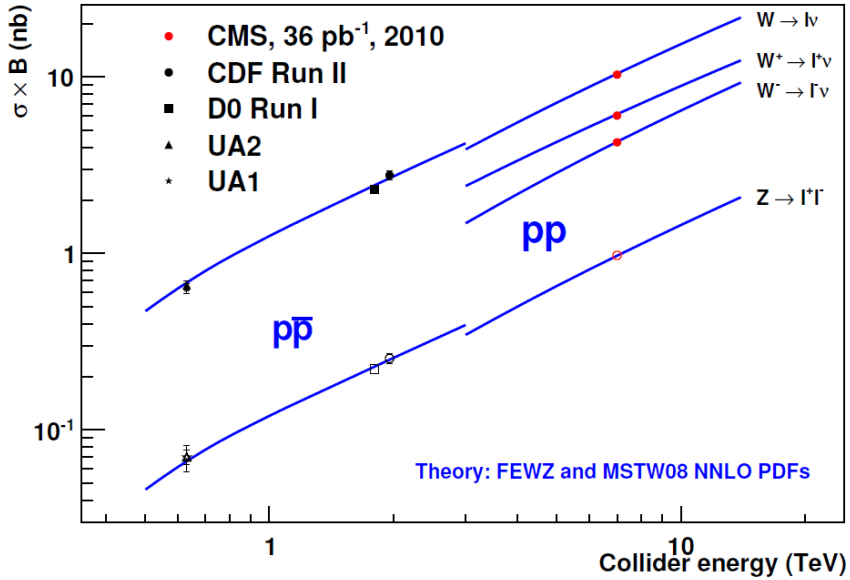

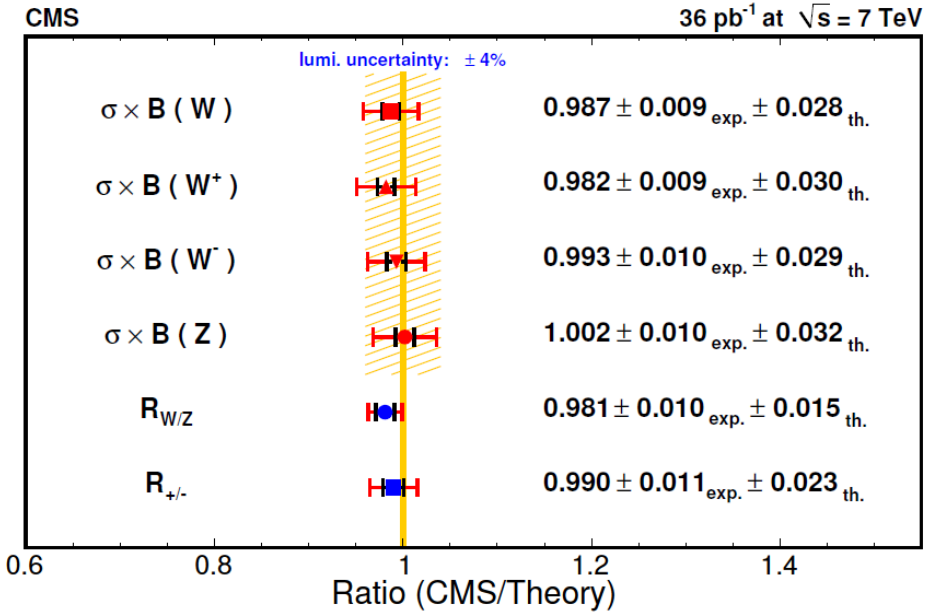

Inclusive Z→ττ cross section (36 pb^{-1})

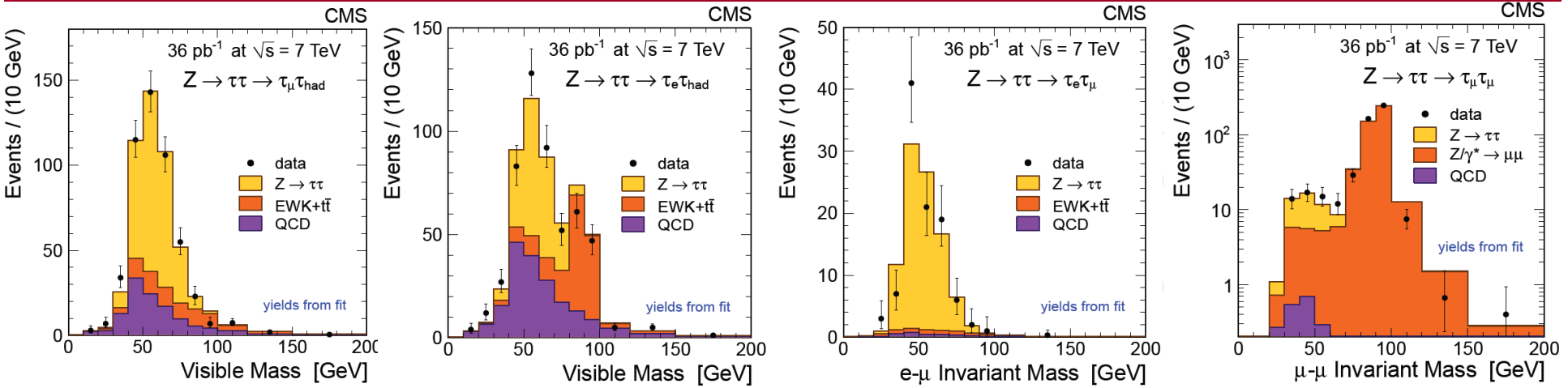

	$\tau_\mu\tau_{had}$	$\tau_e\tau_{had}$	$\tau_e\tau_\mu$	$\tau_\mu\tau_\mu$
Acceptance $\mathcal{A}$	0.128	0.116	0.074	0.163
Selection efficiency ϵ	0.35	0.22	0.55	0.173
Mass window correction f_{out}	0.03	0.03	0.02	0.01
N_{fit}	306	205	90.5	35
Integrated luminosity $\mathcal{L}$ (pb^{-1})	35.7	35.7	35.5	35.7

Dominant systematic: hadronic τ identification efficiency.

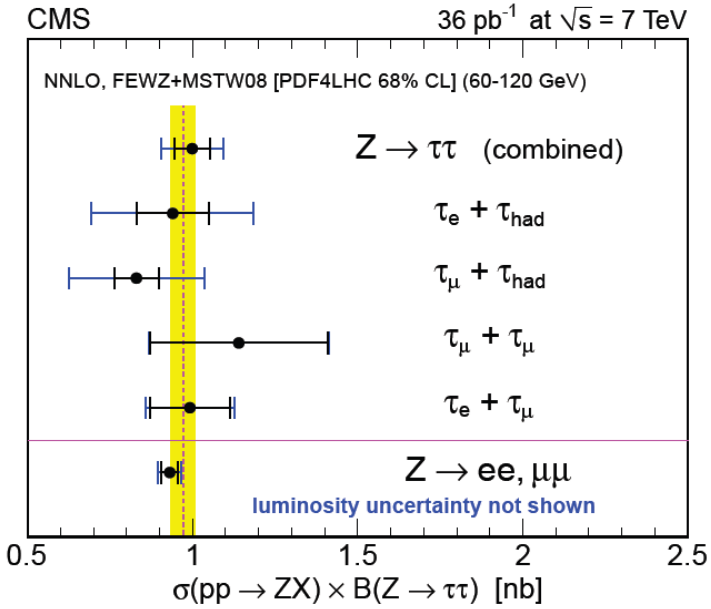

Final state	$\sigma(pp \to ZX) \times \mathcal{B}(Z \to \tau^+\tau^-)$ nb	stat.	syst.	lumi.	τ_{had} − ID
$\tau_\mu\tau_{had}$	0.83	0.07	0.04	0.03	0.19
$\tau_e\tau_{had}$	0.94	0.11	0.03	0.04	0.22
$\tau_e\tau_\mu$	0.99	0.12	0.06	0.04	
$\tau_\mu\tau_\mu$	1.14	0.27	0.04	0.05	

$$\sigma(pp \to ZX) \times \mathcal{B}(Z \to \tau^+\tau^-) = 1.00 \pm 0.05\,(stat.) \pm 0.08\,(syst.) \pm 0.04\,(lumi.)\ nb$$

DY Y in $60<M_{ll}<120$ GeV (36 pb^{-1})

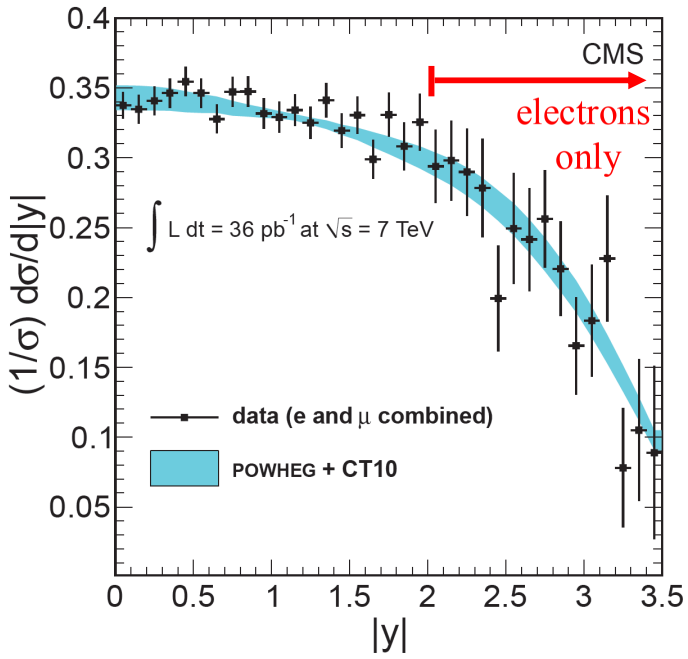

|y| Range	[0.0, 0.1]		[1.8, 1.9]		[3.0, 3.1]
Channel	Muon	Electron	Muon	Electron	Electron
Background Estimation	0.002	0.010	0.002	0.015	0.047
Efficiency Determination	0.003	0.005	0.007	0.007	0.047
Energy/Momentum Scale	0.001	0.004	0.001	0.003	0.009
PDF Acceptance Determination	0.001	0.001	0.001	0.001	0.001
Total	0.004	0.012	0.007	0.017	0.067

Predictions from NLO MSTW08, HERAPDF 1.5, NNPDF 2.0 models are also in agreement with data.

$$x_{\pm} = \frac{m}{\sqrt{s}} e^{\pm y}$$

- |y|-distribution sensitive to PDFs especially in forward region (|y|>2.5) for $4\times10^{-4}<x<0.43$.
- Rapidity y of Z bosons observed to be symmetric about y=0. Ranges of measurements |y|<3.5.
- Measured dσ/d|y| normalized to inclusive Z cross section ➔ canceling sources of systematic uncertainties.
- Agreement between electrons & muons within uncertainties. Measurements are combined with main correlation the (small) PDF uncertainty.
- |y| is corrected for signal acceptance, efficiencies, detector resolution & FSR using unfolding technique.
- Acceptance: from POWHEG + CT10 , Z2 tune for underlying event.

DY Q_T in $60<M_{ll}<120$ GeV (36 pb^{-1})

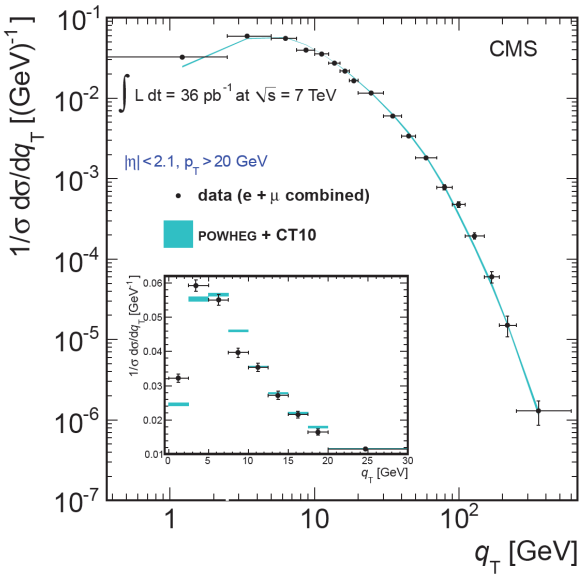

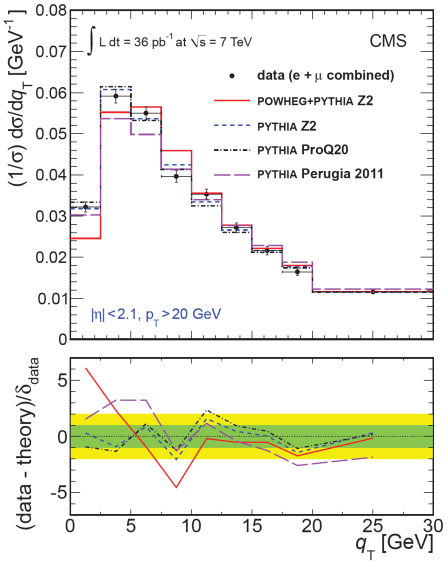

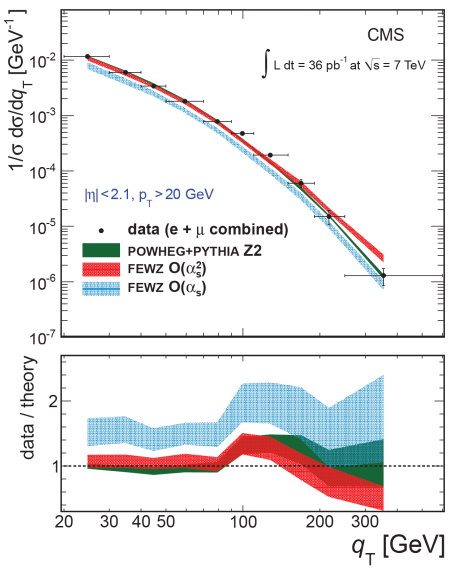

- qT-distribution improves the understanding of the underlying collision process at low qT and tests NNLO pQCD predictions at high qT.
- Ranges of measurements qT<600 GeV, lepton pT > 20 GeV, lepton |η|<2.1 . qT bin size gives sufficient resolution to observe the shape of the distribution, limit bin-migration, enough stats.
- At low qT distribution is determined by non-pQCD, which is modeled by PYTHIA with few free parameters. Several "tunes" were tested. Good agreement is observed only for Z2 and ProQ20.
- At high qT precision determined by pQCD & handling of factorization/renormalization scale dependence. Measurements are compared with POWHEG+PYTHIA Z2 and FEWZ (NNLO).

q_T Range	[2.5 GeV, 5.0 GeV]		[110 GeV, 150 GeV]	
Channel	Muon	Electron	Muon	Electron
Background Estimation	0.004	0.005	0.019	0.028
Efficiency Determination	0.010	0.002	0.010	0.008
Energy Scale	-	0.022	-	0.035
Tracker Alignment	0.015	0.013	0.023	0.020
Unfolding	0.006	0.004	0.017	0.001
PDF Acceptance Determination	0.002	0.002	0.001	0.001
Total	0.020	0.026	0.036	0.050

dσ(Z)/dM (4.5 fb^{-1})

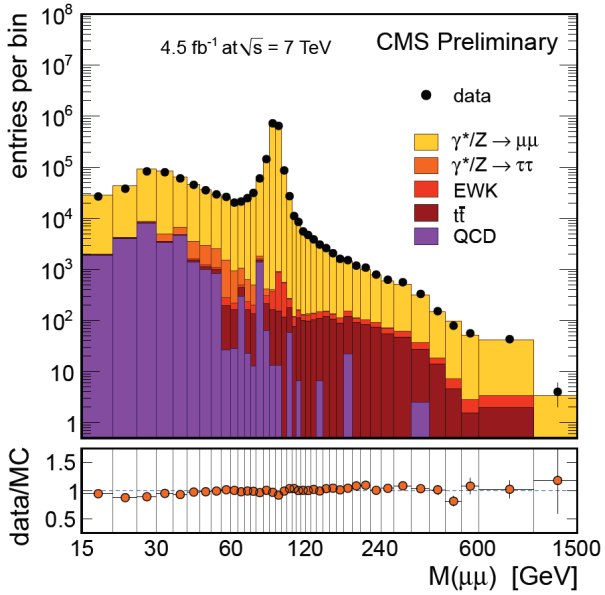

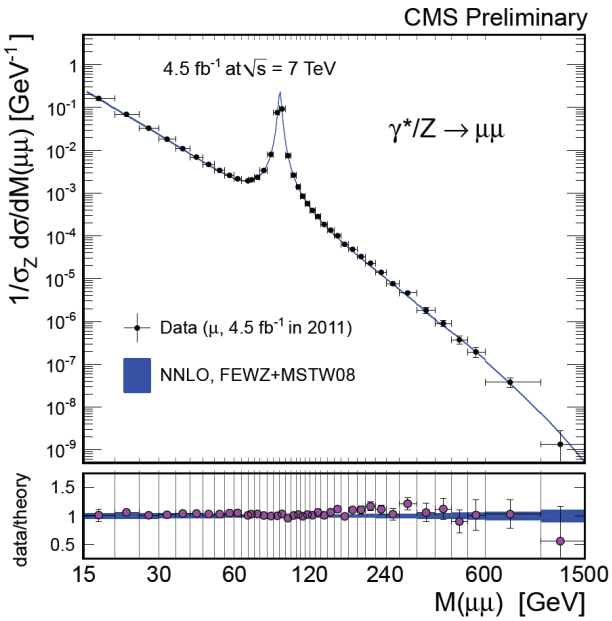

- Tests the pQCD and sets constraints on PDFs. Theoretical predictions established to NNLO.
- Signal MC : POWHEG + FEWZ corrections.
- Measurements normalized to the Z peak (60 – 120 GeV) ➔ cancelation of luminosity uncertainties, reduction of PDF uncertainties on acceptance and efficiency uncertainties.
- Distribution is unfolded for resolution and corrected bin-by-bin for QED FSR.
- Leading systematics
  Electrons : efficiency corrections
  Muons : background estimation

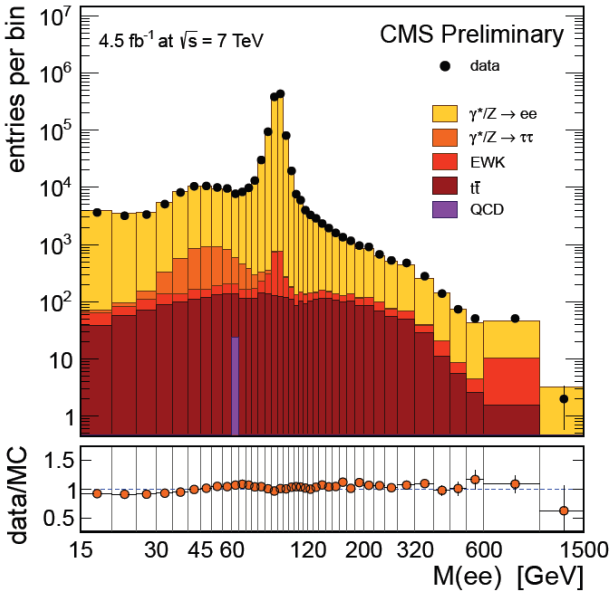

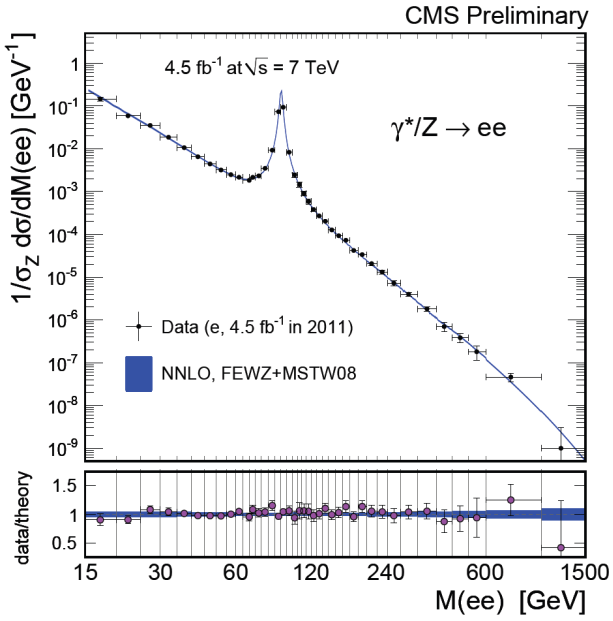

$d^2\sigma(Z)/dMdY$ (muons , 4.5 fb^{-1})

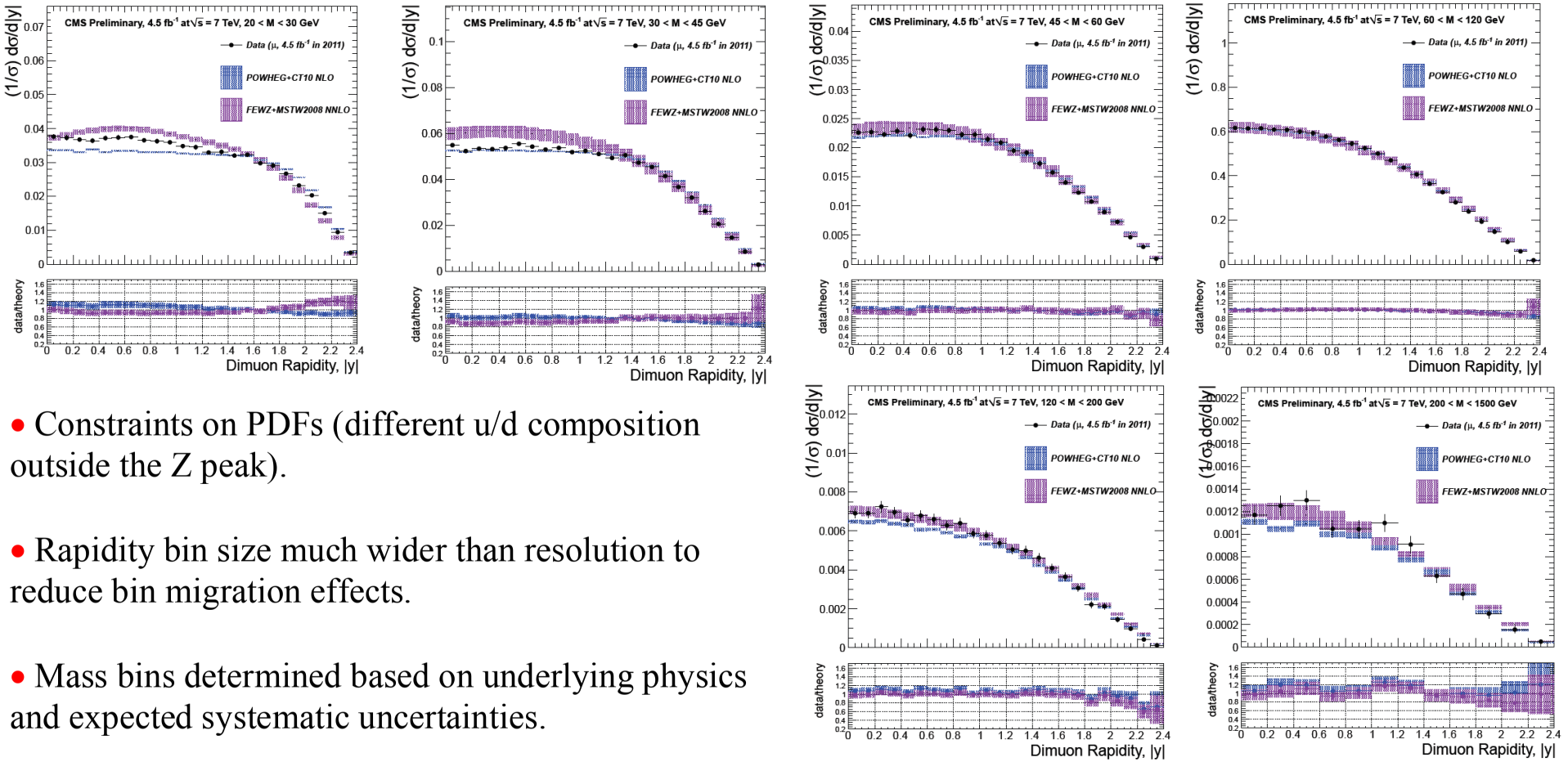

- Constraints on PDFs (different u/d composition outside the Z peak).

- Rapidity bin size much wider than resolution to reduce bin migration effects.

- Mass bins determined based on underlying physics and expected systematic uncertainties.

- Low mass region (20-45) : significant HO QCD & FSR effects ➔ two bins
- Dimuon rapidity resolution increasing at high Y, almost independent of mass range.

- Leading systematic: background estimation; Other sources : muon efficiency & unfolding. Systematic uncertainties increase with dimuon Y & $M_{\mu\mu}$.

A_{FB} of opposite lepton pairs from Z/γ* (4.7 fb^{-1})

Born level, $P_T(l)$>20 GeV, $|\eta(l)|$<2.4

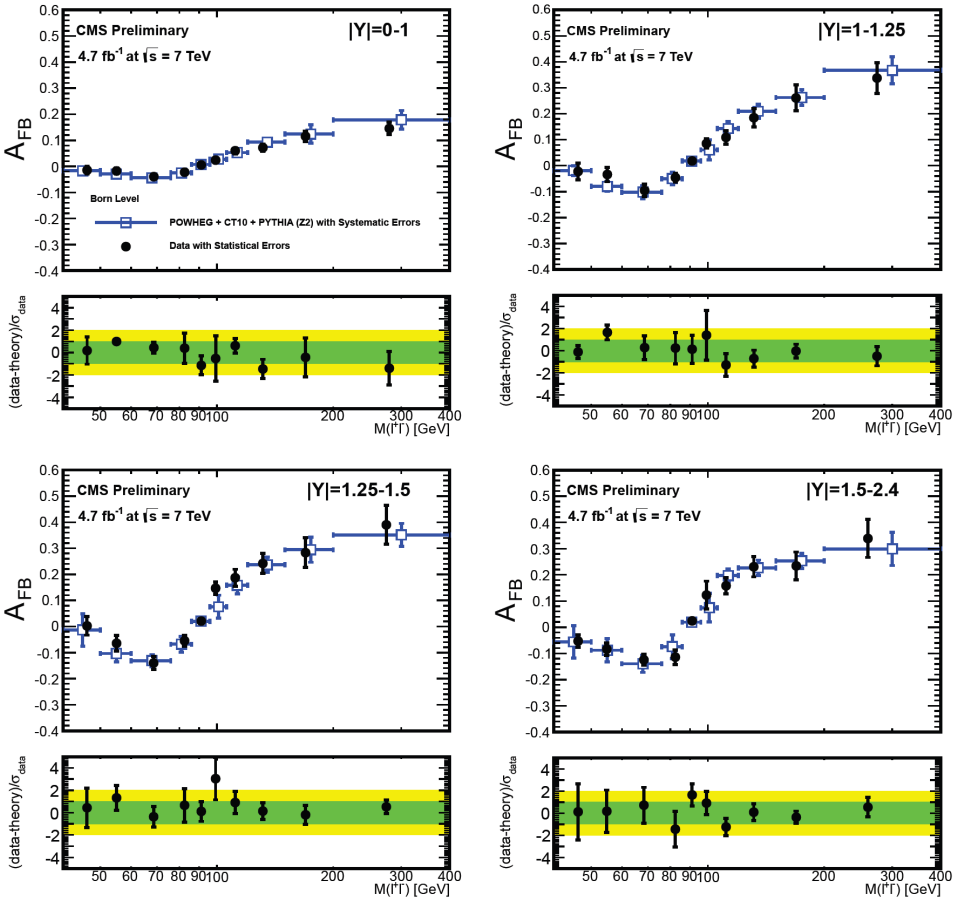

A_{FB} versus di-lepton mass and rapidity.

At a given M_{ll} : $\frac{d\sigma}{d(\cos\theta)} = A(1+\cos^2\theta) + B\cos\theta$

$$A_{FB} = \frac{\sigma_F - \sigma_B}{\sigma_F + \sigma_B} = \frac{3B}{8A}$$

σ_F ($\cos\theta > 0$)
σ_B ($\cos\theta < 0$)

For θ is used the Collins-Soper frame

$$\cos\theta^*_{CS} = \frac{Q_Z}{|Q_Z|}\frac{2(P_l^+P_{\bar{l}}^- - P_l^-P_{\bar{l}}^+)}{|Q|\sqrt{Q^2+Q_T^2}}$$

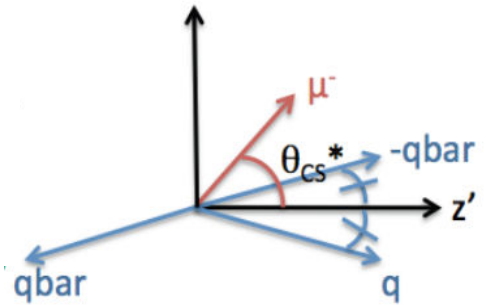

- A_{FB} is small at Z pole due to the small value of the lepton vector coupling constant.
- A_{FB} exhibits characteristic energy dependence, driven by virtual photon and Z interference.

Weak mixing angle (muons ; 1.1 fb^{-1})

Analysis Method: unbinned extended maximum-likelihood fit that simultaneously describes the Signal & Background yields and the parameters of the di-muon rapidity, invariant mass and decay angle (Y, s, cosθ*) distributions.

$$\mathcal{P}_{\rm sig}(Y, \hat{s}, \cos\theta^*; \theta_{\rm eff}) = \mathcal{G}(Y, \hat{s}, \cos\theta^*) \times \int_{-\infty}^{+\infty} dx \mathcal{R}(x) \mathcal{P}_{\rm ideal}(Y, \hat{s} - x, \cos\theta^*; \theta_{\rm eff})$$

Acceptance*Efficiency (G) and mass resolution/FSR (R(x)) convolved with LO generator level distribution P_{ideal} which describes DY process, with the weak mixing angle (θ_{eff}) a fit parameter.

Muons P_T = 18 , 8 GeV, $|\eta|<2.4$, Z qT<25 GeV, $80<M_{\mu\mu}<100$ GeV

$$\sin^2\theta_{\rm eff} = 0.2287 \pm 0.0020\,(\text{stat.}) \pm 0.0025\,(\text{syst.})$$

TABLE II. Corrections to the fit values and systematic uncertainties in the measurement of $\sin^2\theta_{\rm eff}$.

source	correction	uncertainty
PDF	-	±0.0013
FSR	-	±0.0011
LO model (EWK)	-	±0.0002
LO model (QCD)	+0.0012	±0.0012
resolution and alignment	+0.0007	±0.0013
efficiency and acceptance	-	±0.0003
background	-	±0.0001
total	+0.0019	±0.0025

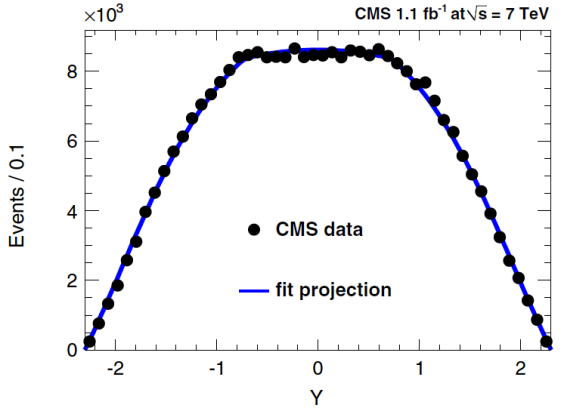

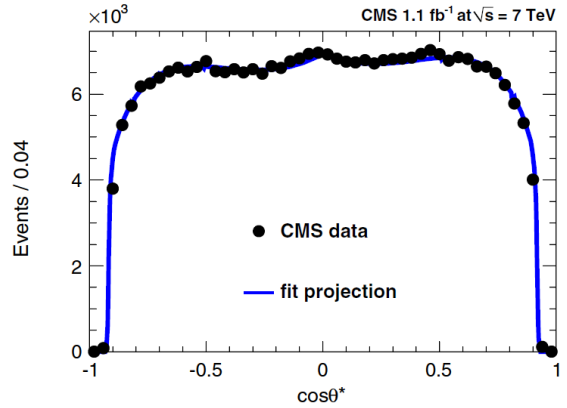

Conclusions

CMS has lunched a broad program of EWK measurements with data from the p-p LHC collisions at 7 TeV. Great variety of measurements that test the SM predictions.

- Precise cross section measurements of inclusive W & Z bosons decaying into electrons, muons and taus.
- Detailed studies of DY deferential & double deferential cross sections.
- Precise measurements of EWK observables (asymmetries, ratios, polarization).

➢ Further constraints of PDFs will be soon available.
➢ Many measurements already systematics limited.

Results are in agreement with theoretical predictions.

We should not forget that …
Precise EWK measurements lay the foundation for new physics beyond the SM.

References

- W & Z inclusive cross sections in electron & muon final states

JHEP10(2011)132

- W→τν cross section

CMS-PAS-EWK-11-019

- W charge asymmetry

CMS-PAS-SMP-12-001, CMS-PAS-EWK-11-005, JHEP04(2011)050

- W polarization

PRL 107, 021802 (2011)

- Z→ττ cross section

JHEP08(2011)117

- Rapidity and transverse momentum distributions of Z bosons

PHYSICAL REVIEW D 85, 032002 (2012)

- Differential & double differential DY cross sections

CMS-PAS-EWK-11-020, CMS-PAS-EWK-11-007, JHEP10(2011)007

- Forward-backward asymmetry of Drell-Yan pairs

CMS-PAS-EWK-11-004, CMS-PAS-EWK-10-011

- Weak mixing angle with the Drell-Yan process

PHYSICAL REVIEW D 84, 112002 (2011)

BACKUP

W & Z production

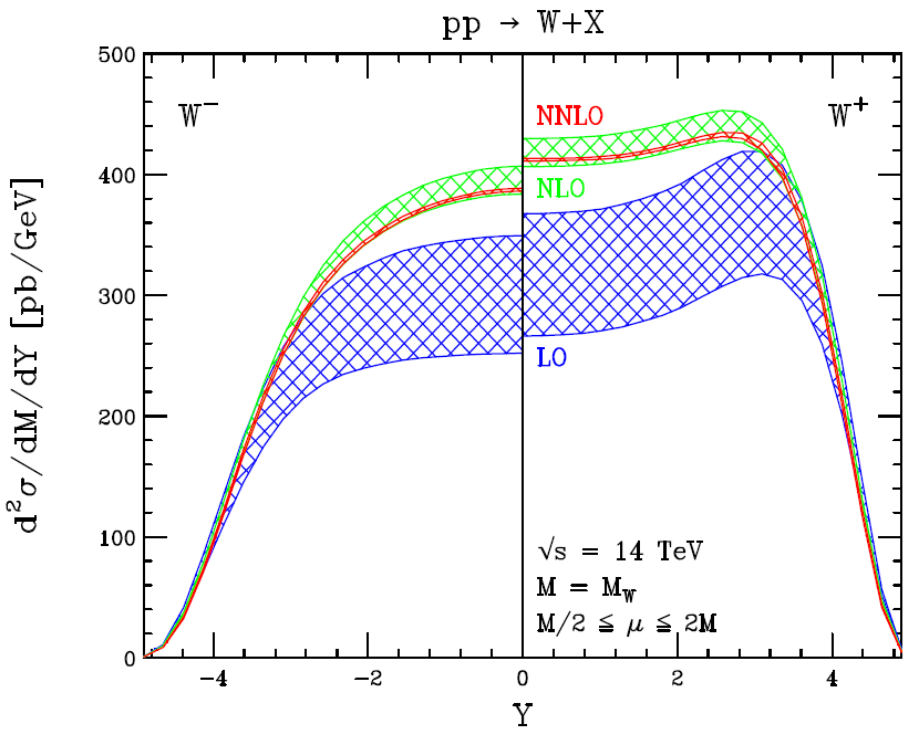

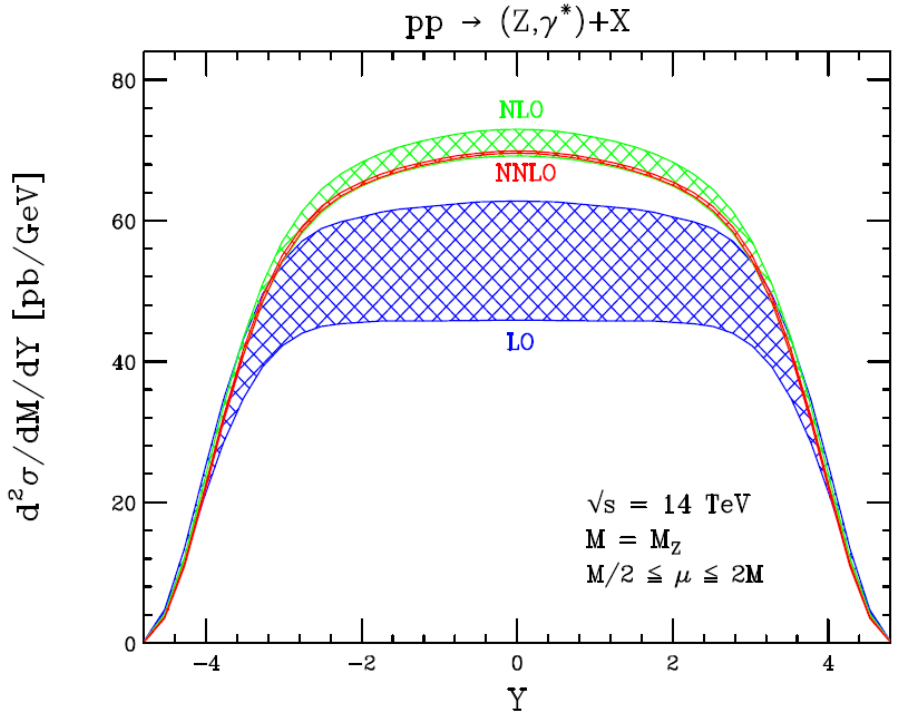

hep-ph/0312266

Inclusive W cross section (36 pb^{-1})

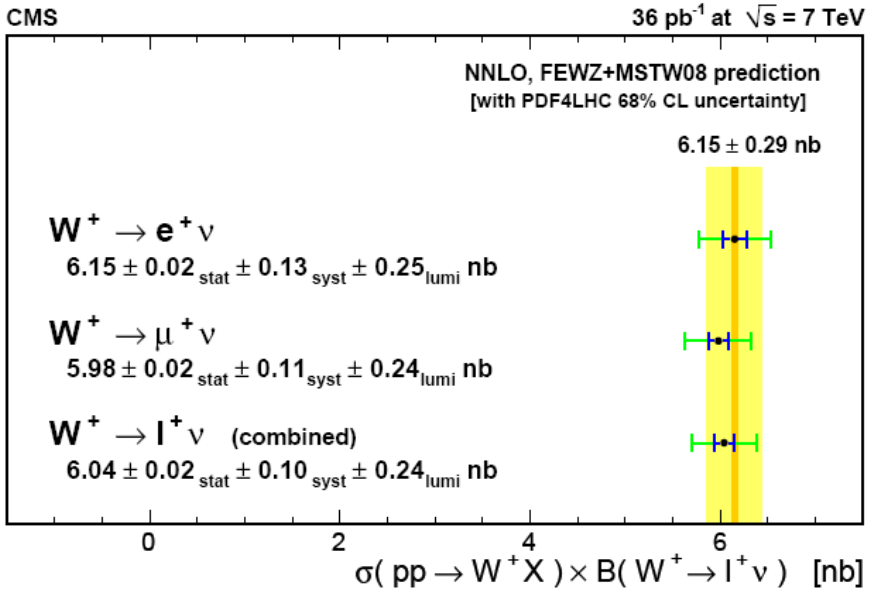

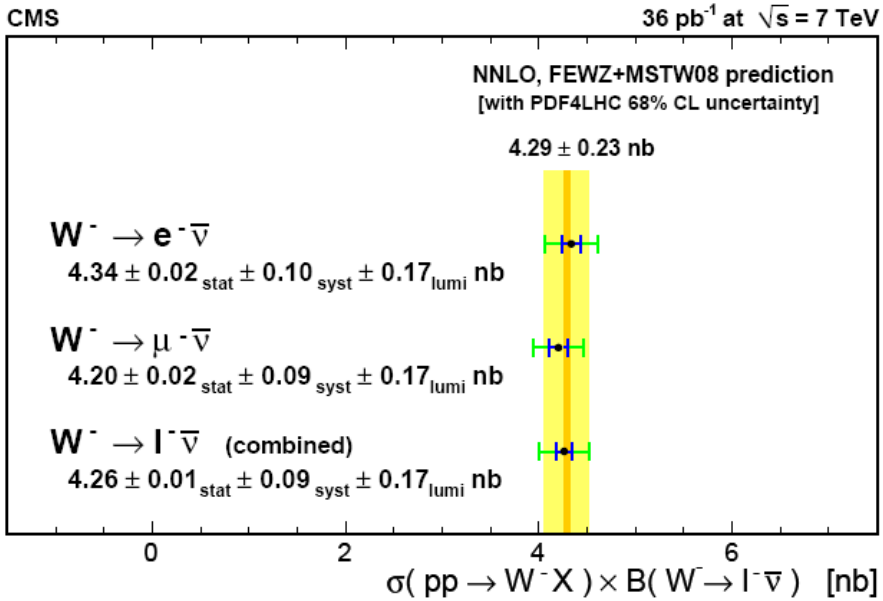

Inclusive $W \rightarrow \tau_{had} \nu$ cross section (32.4 pb^{-1})

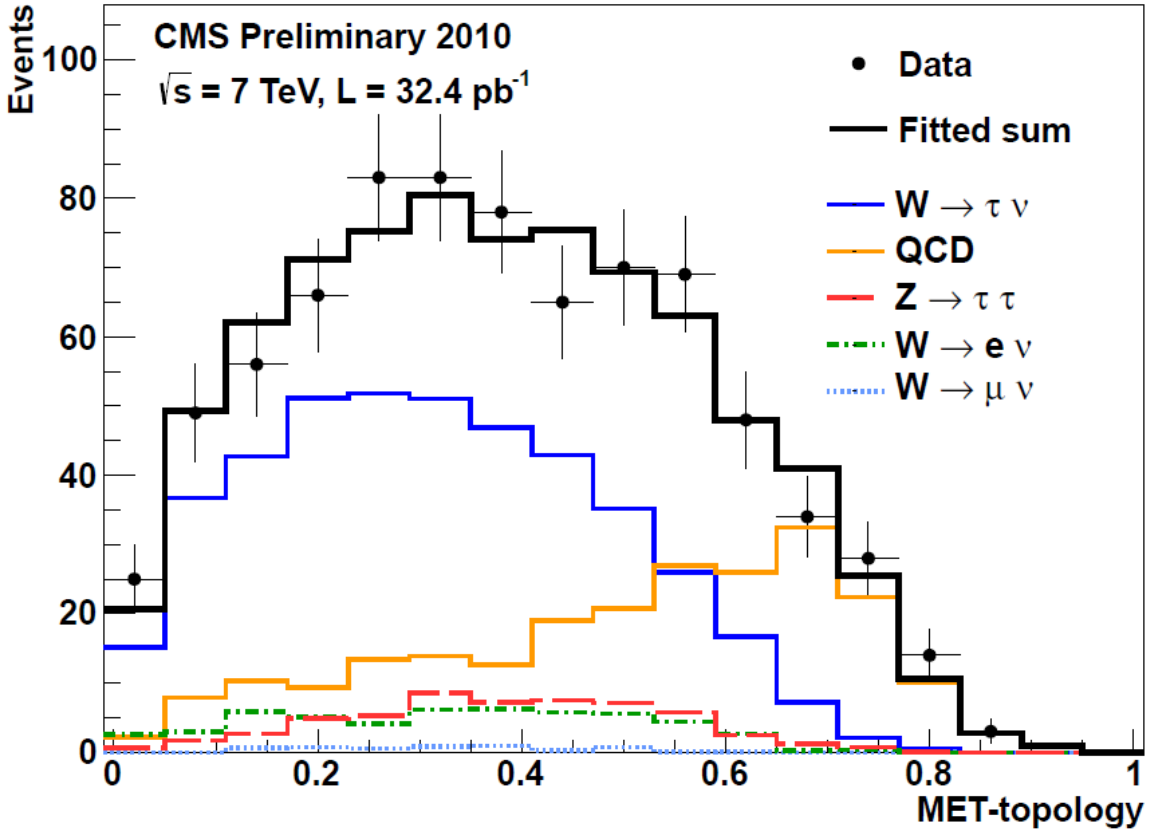

QCD template: Fit the MET topology (T) distribution.
T = ratio between the PT sum of PF-candidates projected in two hemispheres
Hemisphere A : MET direction
Hemisphere B: opposite to MET direction
Good separation in T of signal & bkgd.

W charge asymmetry (electrons; 840 pb^{-1})

Table 1: Summary of the systematic uncertainties. All values are in units $\times 10^{-3}$.

	Signal Yield	Energy Scale and Res.	Charge MisId.	Efficiency Ratio
$0.0 < \|\eta\| < 0.2$	1.8	0.6	0.0	4.5
$0.2 < \|\eta\| < 0.4$	2.5	0.6	0.0	4.4
$0.4 < \|\eta\| < 0.6$	2.7	0.3	0.0	4.4
$0.6 < \|\eta\| < 0.8$	2.5	0.3	0.0	4.4
$0.8 < \|\eta\| < 1.0$	1.9	0.6	0.1	4.4
$1.0 < \|\eta\| < 1.2$	2.4	1.0	0.1	4.9
$1.2 < \|\eta\| < 1.4$	2.6	0.8	0.1	5.4
$1.6 < \|\eta\| < 1.8$	3.1	0.8	0.1	9.2
$1.8 < \|\eta\| < 2.0$	2.0	1.6	0.2	8.7
$2.0 < \|\eta\| < 2.2$	2.0	2.6	0.3	10.0
$2.2 < \|\eta\| < 2.4$	2.9	2.4	0.3	12.5

	Measured Asymmetry ($\mathcal{A}$)	Theory Prediction CT10	HERAPDF	MSTW	NNPDF
$0.0 < \|\eta\| < 0.2$	$102 \pm 3 \pm 5$	109^{+5}_{-5}	106^{+4}_{-8}	83^{+3}_{-5}	107 ± 5
$0.2 < \|\eta\| < 0.4$	$111 \pm 3 \pm 5$	114^{+5}_{-5}	110^{+4}_{-8}	85^{+3}_{-5}	110 ± 5
$0.4 < \|\eta\| < 0.6$	$116 \pm 3 \pm 5$	119^{+5}_{-5}	115^{+4}_{-8}	92^{+3}_{-5}	116 ± 5
$0.6 < \|\eta\| < 0.8$	$123 \pm 3 \pm 5$	126^{+5}_{-5}	122^{+4}_{-8}	98^{+3}_{-5}	123 ± 5
$0.8 < \|\eta\| < 1.0$	$133 \pm 3 \pm 5$	138^{+5}_{-6}	132^{+4}_{-8}	108^{+4}_{-5}	134 ± 5
$1.0 < \|\eta\| < 1.2$	$136 \pm 3 \pm 6$	146^{+6}_{-6}	140^{+5}_{-8}	120^{+4}_{-5}	145 ± 5
$1.2 < \|\eta\| < 1.4$	$156 \pm 3 \pm 6$	164^{+6}_{-7}	153^{+5}_{-7}	136^{+5}_{-5}	158 ± 5
$1.6 < \|\eta\| < 1.8$	$166 \pm 3 \pm 10$	195^{+8}_{-9}	181^{+5}_{-5}	168^{+5}_{-5}	190 ± 4
$1.8 < \|\eta\| < 2.0$	$197 \pm 3 \pm 9$	207^{+8}_{-10}	196^{+4}_{-3}	184^{+6}_{-5}	206 ± 4
$2.0 < \|\eta\| < 2.2$	$224 \pm 3 \pm 11$	224^{+8}_{-11}	211^{+5}_{-3}	198^{+6}_{-5}	219 ± 4
$2.2 < \|\eta\| < 2.4$	$210 \pm 4 \pm 13$	241^{+8}_{-12}	225^{+9}_{-4}	214^{+6}_{-5}	231 ± 5

The full covariance systematic errors matrix

	[0.0, 0.2]	[0.2, 0.4]	[0.4, 0.6]	[0.6, 0.8]	[0.8, 1.0]	[1.0, 1.2]	[1.2, 1.4]	[1.6, 1.8]	[1.8, 2.0]	[2.0, 2.2]	[2.2, 2.4]
[0.0, 0.2]	23.7	2.6	2.2	2.5	2.7	2.9	2.9	2.9	2.8	3.1	4.2
[0.2, 0.4]	2.6	26.2	2.6	2.9	3.1	3.3	3.4	3.2	3.0	3.9	4.7
[0.4, 0.6]	2.2	2.6	26.6	2.6	2.8	2.9	3.2	2.9	2.5	3.3	4.1
[0.6, 0.8]	2.5	2.9	2.6	25.6	3.3	3.4	3.7	3.3	2.8	3.7	4.7
[0.8, 1.0]	2.7	3.1	2.8	3.3	23.3	3.9	4.2	3.7	3.4	4.6	5.6
[1.0, 1.2]	2.9	3.3	2.9	3.4	3.9	30.8	4.5	4.1	4.0	5.7	6.8
[1.2, 1.4]	2.9	3.4	3.2	3.7	4.2	4.5	36.5	4.3	3.7	5.8	6.7
[1.6, 1.8]	2.9	3.2	2.9	3.3	3.7	4.1	4.3	94.9	3.8	5.1	6.2
[1.8, 2.0]	2.8	3.0	2.5	2.8	3.4	4.0	3.7	3.8	82.4	6.2	7.0
[2.0, 2.2]	3.1	3.9	3.3	3.7	4.6	5.7	5.8	5.1	6.2	110.7	10.3
[2.2, 2.4]	4.2	4.7	4.1	4.7	5.6	6.8	6.7	6.2	7.0	10.3	171.0

W Charge Asymmetry (Muons ; 234 pb^{-1})

$\|\eta\|$ bin	Sig.& Bkg. Estim.	Eff. Ratio	Muon Scale	Total
[0.00, 0.20]	0.22	0.25	0.25	0.41
[0.20, 0.40]	0.23	0.26	0.25	0.43
[0.40, 0.60]	0.25	0.25	0.25	0.44
[0.60, 0.80]	0.28	0.26	0.25	0.46
[0.80, 1.00]	0.33	0.29	0.25	0.50
[1.00, 1.20]	0.37	0.30	0.25	0.54
[1.20, 1.40]	0.42	0.32	0.25	0.58
[1.40, 1.60]	0.47	0.33	0.25	0.63
[1.60, 1.85]	0.49	0.33	0.25	0.64
[1.85, 2.10]	0.53	0.39	0.25	0.70
[2.10, 2.40]	0.58	1.10	0.85	1.50

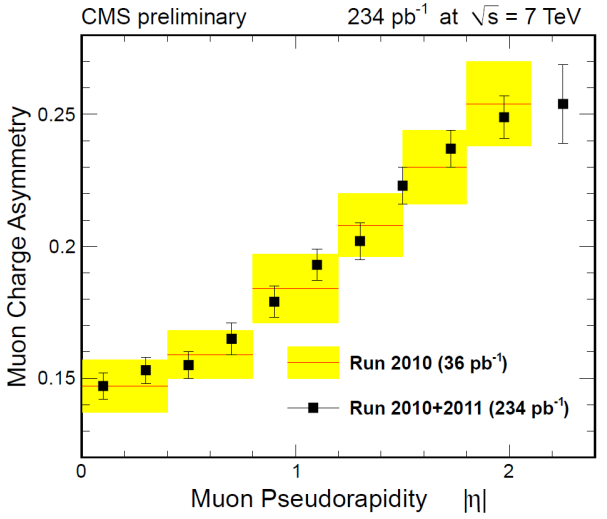

$\|\eta\|$ bin	$\mathcal{A} \pm \text{stat} \pm \text{sys}$
[0.00, 0.20]	14.7±0.32±0.41
[0.20, 0.40]	15.3±0.33±0.43
[0.40, 0.60]	15.5±0.32±0.44
[0.60, 0.80]	16.5±0.32±0.46
[0.80, 1.00]	17.9±0.34±0.50
[1.00, 1.20]	19.3±0.34±0.54
[1.20, 1.40]	20.2±0.33±0.58
[1.40, 1.60]	22.3±0.34±0.63
[1.60, 1.85]	23.7±0.31±0.64
[1.85, 2.10]	24.9±0.32±0.70
[2.10, 2.40]	25.4±0.35±1.50

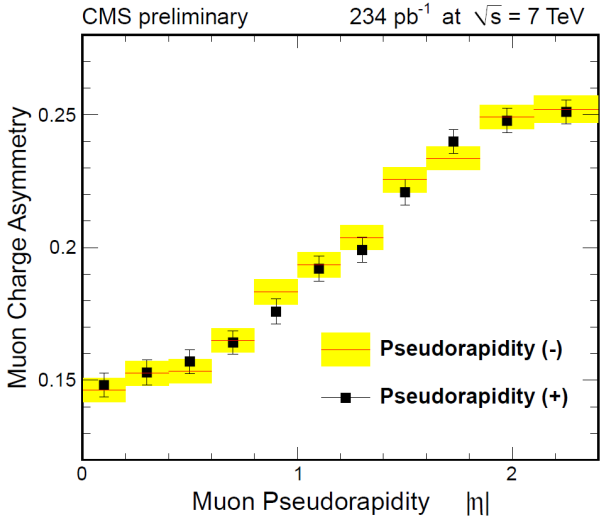

W polarization (36 pb^{-1})

TABLE I. A summary of the individual and combined fit results for negatively charged and positively charged electrons and muons. Systematic uncertainties from different sources are combined in quadrature.

	Fit result
$e : (f_L - f_R)^-$	0.187 ± 0.069 (stat.) ± 0.066 (syst.)
$e : f_0^-$	0.130 ± 0.200 (stat.) ± 0.174 (syst.)
Correlation	-0.204 (stat.), -0.283 (stat. + syst.)
$e : (f_L - f_R)^+$	0.277 ± 0.060 (stat.) ± 0.050 (syst.)
$e : f_0^+$	0.240 ± 0.190 (stat.) ± 0.090 (syst.)
Correlation	-0.295 (stat.), 0.001 (stat. + syst.)
$\mu : (f_L - f_R)^-$	0.240 ± 0.036 (stat.) ± 0.031 (syst.)
$\mu : f_0^-$	0.183 ± 0.087 (stat.) ± 0.123 (syst.)
Correlation	0.395 (stat.), -0.308 (stat. + syst.)
$\mu : (f_L - f_R)^+$	0.310 ± 0.036 (stat.) ± 0.017 (syst.)
$\mu : f_0^+$	0.171 ± 0.085 (stat.) ± 0.099 (syst.)
Correlation	-0.721 (stat.), -0.269 (stat. + syst.)
Combined: $(f_L - f_R)^-$	0.226 ± 0.031 (stat.) ± 0.050 (syst.)
Combined: f_0^-	0.162 ± 0.078 (stat.) ± 0.136 (syst.)
Correlation	0.304 (stat.), -0.326 (stat. + syst.)
Combined: $(f_L - f_R)^+$	0.300 ± 0.031 (stat.) ± 0.034 (syst.)
Combined: f_0^+	0.192 ± 0.075 (stat.) ± 0.089 (syst.)
Correlation	-0.660 (stat.), -0.121 (stat. + syst.)

TABLE II. Summary of the leading systematic uncertainties for the electron and muon final states, as well as for the combined measurement. The total systematic uncertainties are also shown for reference.

Uncertainty	$(f_L - f_R)^-$	f_0^-	$(f_L - f_R)^+$	f_0^+
	Electron channel			
Recoil energy scale	± 0.042	± 0.150	± 0.027	± 0.078
Recoil resolution	± 0.046	± 0.047	± 0.037	± 0.039
Electron scale	± 0.017	± 0.014	± 0.019	± 0.016
Total uncertainty	± 0.066	± 0.174	± 0.050	± 0.090
	Muon channel			
Recoil energy scale	± 0.029	± 0.123	± 0.011	± 0.092
Recoil resolution	± 0.012	± 0.006	± 0.012	± 0.004
Muon scale	± 0.002	± 0.007	± 0.004	± 0.008
Total uncertainty	± 0.031	± 0.123	± 0.017	± 0.099
	Combined measurement			
Recoil energy scale	± 0.033	± 0.133	± 0.016	± 0.087
Recoil resolution	± 0.035	± 0.023	± 0.027	± 0.015
Electron scale	± 0.013	± 0.011	± 0.012	± 0.008
Muon scale	± 0.002	± 0.004	± 0.004	± 0.004
Total uncertainty	± 0.050	± 0.136	± 0.034	± 0.089

W polarization (36 pb^{-1})

The cross section for W production : $dN/d\Omega \sim (1 + \cos^2\theta^*) + \Sigma_{(i=0,4)} A_i F_i(\theta^*,\varphi^*)$,
A_i **depend** on W **charge**, **PT** , **Y** and make up the elements of the **polarization density matrix**.

If we integrate over φ* then: $$\frac{dN}{d\cos\theta^*} \propto (1 + \cos^2\theta^*) + \frac{1}{2}A_0(1 - 3\cos^2\theta^*) + A_4\cos\theta^*.$$

f_L, f_R, f_0 are related to A_0 & A_4 as $\mathbf{A_0 \sim f_0}$ & $\mathbf{A_4 \sim (f_R - f_L)}$

f_i parameters **are not expected to be the same** for **both charges** (ratio of valence u quarks to sea quarks is higher than that for valence d quarks).

The amount of W boson momentum imparted to the **charged decay lepton** is determined by **cosθ***, and hence an asymmetry in the cosθ* distribution **leads** to an asymmetry between the neutrino and charged-lepton momentum spectra. Quantified via a measurement of the A_4 parameter.

Polarization and correlation of L_P with cosθ* **increase** with pT(W); Statistics **decreases** sharply with pT(W); **pT(W) > 50 GeV** optimum based on the expected statistical uncertainty of the (f_L - f_R) measurement.

Simulation: MADGRAPH + CTEQ6L

(f_L - f_R) and f_0 are measured by using a binned maximum likelihood fit to the LP variable, separately for W^+ and W^- bosons in the electron and muon final states. The L_P distribution for each of the three polarization states of the W boson is extracted from simulation.

As high-pT W bosons are also produced in top quark decays, **only events** with **up to three reconstructed jets are retained**. Jets: PF , PT > 30 GeV, |η|<5, clustered by using the anti-KT algorithm with DR = 0.5

Main **systematic uncertainties**: energy scale and resolution uncertainties of the recoiling jets

DYNNLO+NNPDF21 & CMS+LHCb with muons

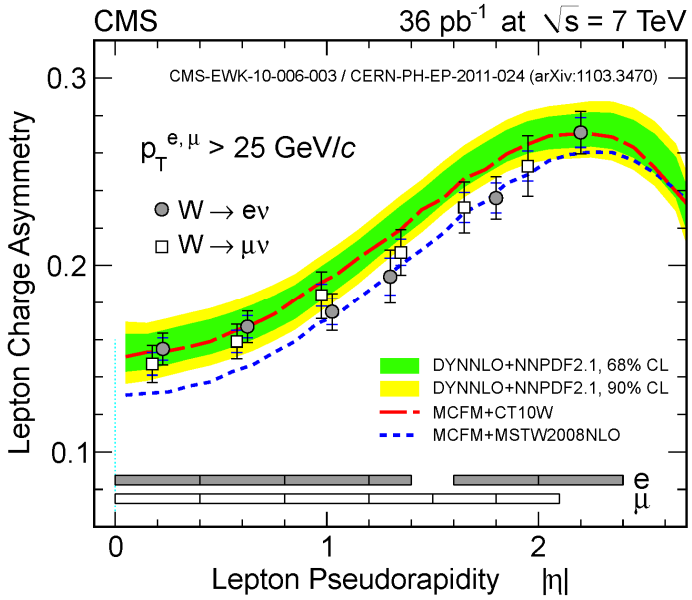

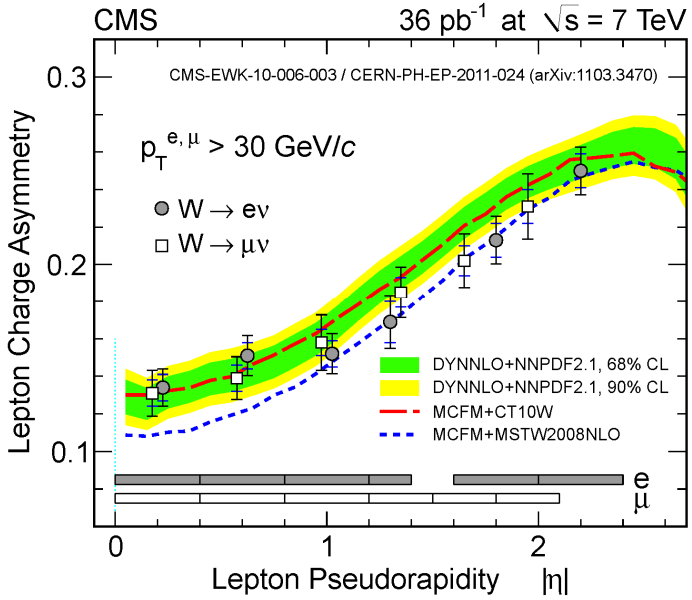

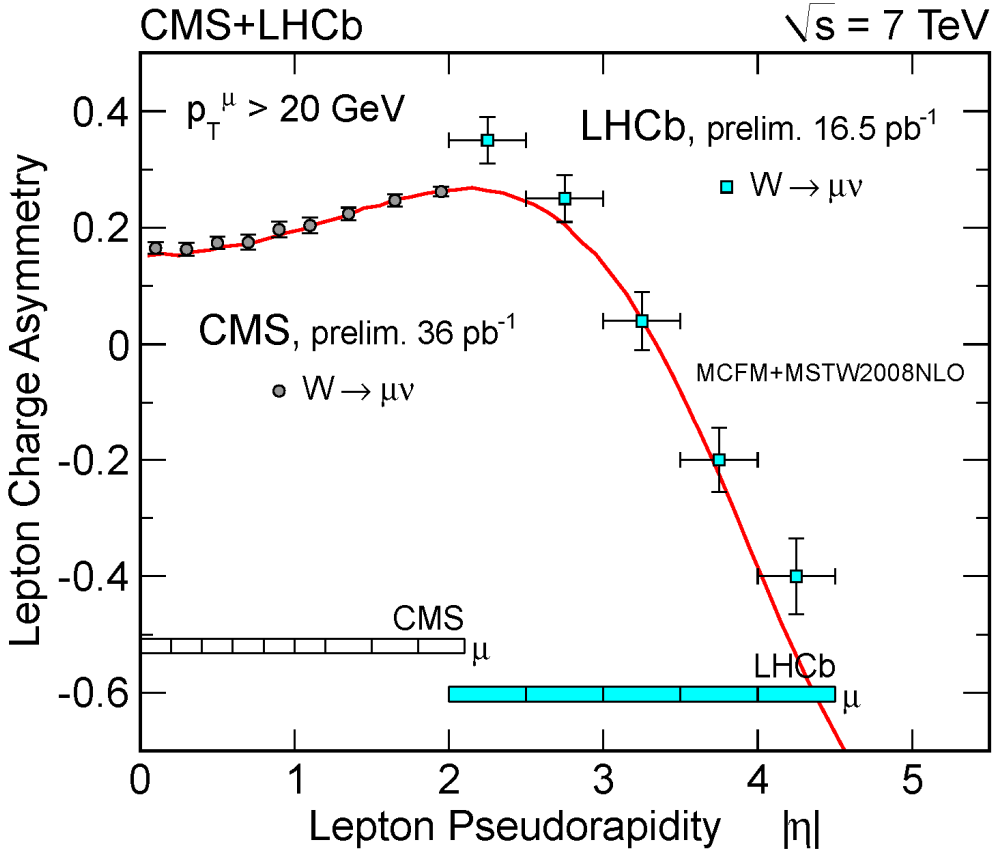

DY Y & Q_T in $60<M_{ll}<120$ GeV (36 pb^{-1})

TABLE II. Measurement of the normalized differential cross section ($\frac{1}{\sigma}\frac{d\sigma}{d|y|}$) for Drell–Yan lepton pairs in the Z-boson mass region ($60 < M_{\ell\ell} < 120$ GeV) as a function of the absolute value of rapidity, separately for the muon and electron channels and combined. Detector geometry and trigger uniformity requirements limit the muon channel measurement to $|y| < 2.0$. The uncertainties shown are the combined statistical and systematic uncertainties.

	Normalized Differential Cross Section		
$\|y\|$ Range	Muon	Electron	Combined
[0.0, 0.1]	0.324 ± 0.012	0.359 ± 0.015	0.337 ± 0.010
[0.1, 0.2]	0.338 ± 0.013	0.326 ± 0.016	0.335 ± 0.010
[0.2, 0.3]	0.338 ± 0.013	0.344 ± 0.017	0.341 ± 0.010
[0.3, 0.4]	0.341 ± 0.013	0.355 ± 0.017	0.346 ± 0.010
[0.4, 0.5]	0.363 ± 0.013	0.339 ± 0.017	0.354 ± 0.011
[0.6, 0.7]	0.312 ± 0.013	0.360 ± 0.018	0.328 ± 0.010
[0.7, 0.8]	0.354 ± 0.013	0.331 ± 0.018	0.347 ± 0.011
[0.8, 0.9]	0.343 ± 0.014	0.355 ± 0.018	0.347 ± 0.011
[0.9, 1.0]	0.332 ± 0.014	0.332 ± 0.018	0.332 ± 0.011
[1.0, 1.1]	0.336 ± 0.014	0.316 ± 0.018	0.329 ± 0.011
[1.1, 1.2]	0.324 ± 0.014	0.352 ± 0.019	0.334 ± 0.011
[1.2, 1.3]	0.321 ± 0.014	0.332 ± 0.019	0.325 ± 0.011
[1.3, 1.4]	0.355 ± 0.016	0.321 ± 0.019	0.341 ± 0.012
[1.4, 1.5]	0.326 ± 0.016	0.313 ± 0.019	0.319 ± 0.012
[1.5, 1.6]	0.331 ± 0.018	0.330 ± 0.020	0.330 ± 0.013
[1.6, 1.7]	0.294 ± 0.018	0.306 ± 0.022	0.299 ± 0.014
[1.7, 1.8]	0.331 ± 0.021	0.332 ± 0.024	0.331 ± 0.016
[1.8, 1.9]	0.324 ± 0.025	0.294 ± 0.024	0.308 ± 0.017
[1.9, 2.0]	0.328 ± 0.032	0.328 ± 0.026	0.328 ± 0.020
[2.0, 2.1]		0.294 ± 0.027	0.294 ± 0.027
[2.1, 2.2]		0.298 ± 0.029	0.298 ± 0.029
[2.2, 2.3]		0.290 ± 0.031	0.290 ± 0.031
[2.3, 2.4]		0.278 ± 0.035	0.278 ± 0.035
[2.4, 2.5]		0.199 ± 0.038	0.199 ± 0.038
[2.5, 2.6]		0.249 ± 0.040	0.249 ± 0.040
[2.6, 2.7]		0.241 ± 0.037	0.241 ± 0.037
[2.7, 2.8]		0.256 ± 0.035	0.256 ± 0.035
[2.8, 2.9]		0.221 ± 0.034	0.221 ± 0.034
[2.9, 3.0]		0.165 ± 0.035	0.165 ± 0.035
[3.0, 3.1]		0.183 ± 0.040	0.183 ± 0.040
[3.1, 3.2]		0.228 ± 0.045	0.228 ± 0.045
[3.2, 3.3]		0.078 ± 0.043	0.078 ± 0.043
[3.3, 3.4]		0.105 ± 0.051	0.105 ± 0.051
[3.4, 3.5]		0.089 ± 0.062	0.089 ± 0.062

TABLE III. Measurement of the normalized differential cross section for Drell–Yan lepton pairs in the Z-boson mass region ($60 < M_{\ell\ell} < 120$ GeV) as a function of q_T, separately for muon and electron channels and for the combination of the two channels. The distribution is normalized by the cross section for Z bosons with both leptons having $|\eta| < 2.1$ and $p_T > 20$ GeV. The uncertainties listed in the table are the combined statistical and systematic uncertainties.

q_T Range (GeV)	Muon Channel	Electron Channel	Combination
[0.0, 2.5]	$(3.21 \pm 0.14) \times 10^{-2}$	$(3.24 \pm 0.25) \times 10^{-2}$	$(3.22 \pm 0.13) \times 10^{-2}$
[2.5, 5.0]	$(5.89 \pm 0.21) \times 10^{-2}$	$(6.03 \pm 0.32) \times 10^{-2}$	$(5.92 \pm 0.17) \times 10^{-2}$
[5.0, 7.5]	$(5.51 \pm 0.20) \times 10^{-2}$	$(5.32 \pm 0.32) \times 10^{-2}$	$(5.50 \pm 0.16) \times 10^{-2}$
[7.5, 10.0]	$(3.90 \pm 0.18) \times 10^{-2}$	$(4.20 \pm 0.30) \times 10^{-2}$	$(3.96 \pm 0.14) \times 10^{-2}$
[10.0,12.5]	$(3.49 \pm 0.16) \times 10^{-2}$	$(3.60 \pm 0.28) \times 10^{-2}$	$(3.53 \pm 0.12) \times 10^{-2}$
[12.5, 15.0]	$(2.74 \pm 0.15) \times 10^{-2}$	$(2.70 \pm 0.25) \times 10^{-2}$	$(2.72 \pm 0.12) \times 10^{-2}$
[15.0, 17.5]	$(2.23 \pm 0.14) \times 10^{-2}$	$(2.00 \pm 0.22) \times 10^{-2}$	$(2.16 \pm 0.10) \times 10^{-2}$
[17.5, 20.0]	$(1.68 \pm 0.12) \times 10^{-2}$	$(1.59 \pm 0.20) \times 10^{-2}$	$(1.65 \pm 0.09) \times 10^{-2}$
[20.0, 30.0]	$(1.14 \pm 0.04) \times 10^{-2}$	$(1.20 \pm 0.05) \times 10^{-2}$	$(1.16 \pm 0.04) \times 10^{-2}$
[30.0, 40.0]	$(6.32 \pm 0.28) \times 10^{-3}$	$(5.62 \pm 0.31) \times 10^{-3}$	$(5.98 \pm 0.27) \times 10^{-3}$
[40.0, 50.0]	$(3.53 \pm 0.21) \times 10^{-3}$	$(3.18 \pm 0.24) \times 10^{-3}$	$(3.38 \pm 0.18) \times 10^{-3}$
[50.0, 70.0]	$(1.74 \pm 0.10) \times 10^{-3}$	$(1.90 \pm 0.12) \times 10^{-3}$	$(1.81 \pm 0.09) \times 10^{-3}$
[70.0, 90.0]	$(7.76 \pm 0.71) \times 10^{-4}$	$(7.86 \pm 0.77) \times 10^{-4}$	$(7.79 \pm 0.54) \times 10^{-4}$
[90.0, 110.0]	$(4.87 \pm 0.55) \times 10^{-4}$	$(4.57 \pm 0.59) \times 10^{-4}$	$(4.75 \pm 0.42) \times 10^{-4}$
[110.0, 150.0]	$(1.79 \pm 0.22) \times 10^{-4}$	$(2.18 \pm 0.26) \times 10^{-4}$	$(1.93 \pm 0.17) \times 10^{-4}$
[150.0, 190.0]	$(7.10 \pm 1.40) \times 10^{-5}$	$(4.82 \pm 1.31) \times 10^{-5}$	$(6.00 \pm 0.99) \times 10^{-5}$
[190.0, 250.0]	$(1.17 \pm 0.51) \times 10^{-5}$	$(2.05 \pm 0.64) \times 10^{-5}$	$(1.51 \pm 0.43) \times 10^{-5}$
[250.0, 600.0]	$(2.24 \pm 0.78) \times 10^{-6}$	$(0.81 \pm 0.52) \times 10^{-6}$	$(1.29 \pm 0.44) \times 10^{-6}$

AFB

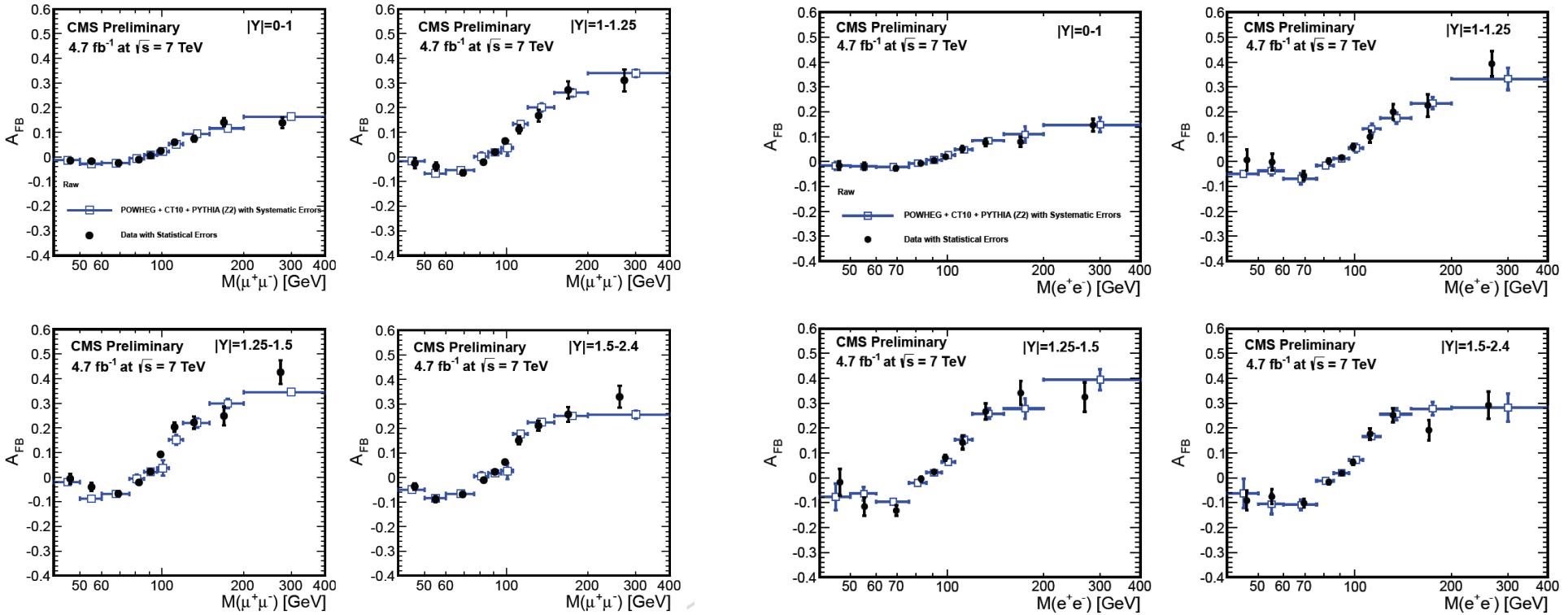

raw AFB for muons

raw AFB for electrons